

# For Reference

---

NOT TO BE TAKEN FROM THIS ROOM

For Reference

NOT TO BE TAKEN FROM THIS ROOM

EX LIBRIS  
UNIVERSITATIS  
ALBERTAENSIS





Digitized by the Internet Archive  
in 2019 with funding from  
University of Alberta Libraries

<https://archive.org/details/Singhal1965>









765 2  
125717  
x 136

THE UNIVERSITY OF ALBERTA

LABORATORY SIMULATION OF UNCONSOLIDATED POROUS MEDIA

BY

ASHOK K. SINGHAL

A THESIS

SUBMITTED TO THE FACULTY OF GRADUATE STUDIES  
IN PARTIAL FULFILMENT OF THE REQUIREMENTS FOR THE  
DEGREE OF MASTER OF SCIENCE

IN

PETROLEUM ENGINEERING

DEPARTMENT OF CHEMICAL AND PETROLEUM ENGINEERING

EDMONTON, ALBERTA

SEPTEMBER, 1965



UNIVERSITY OF ALBERTA  
FACULTY OF GRADUATE STUDIES

The undersigned certify that they have read, and recommend to the Faculty of Graduate Studies for acceptance, a thesis entitled "Laboratory Simulation of Unconsolidated Porous Media" submitted by Ashok K. Singhal in partial fulfilment of the requirements for the degree of Master of Science in Petroleum Engineering.



## ACKNOWLEDGEMENTS

The author wishes to express his sincere thanks to Professor P.M. Dranchuk, Department of Chemical and Petroleum Engineering, University of Alberta, under whose guidance the main part of this project was carried out, and to Professor W. Nader, who suggested the problem, gave valuable advice and helped a great deal in the designing of the equipment and the supervision of its construction.

The author also expresses thanks to the technical staff of the Chemical and Petroleum Engineering shop and store for their cooperation and assistance in design and construction of the equipment.

The financial assistance of the National Research Council and the University of Alberta, which made this work possible, is gratefully acknowledged





## ABSTRACT

In various laboratory studies in the field of Petroleum Engineering it is necessary to simulate natural porous media by means of packed models. It is often necessary to conduct several tests on the same model, starting with identical initial conditions. Therefore, it is necessary, after each test, either to return the model to its original state, or to prepare another model with properties identical to that of its predecessor. Although it is usually best to choose the former, there are occasions when this is physically impossible. Consequently there is a great need for a method of reproducing packed models.

In Part I of the study described herein, an attempt was made to control both porosity and permeability of packed models. The technique employed consisted of packing non-cohesive particles into a cell with the aid of compaction and vibration. The results suggest that the porosity of a pack decreases with increase in particle size as well as with amplitude of vibration. However, the technique appears to be inadequate for controlling permeability.

Part II of the study consisted of an examination of techniques for the application of a silicone fluid and hexamethyldisilazane (HMDS) to the surface of glass beads, so as to effect a controlled change in their wettability characteristics. Iso-octane and NaCl brine served as the oil and water



phases, respectively and the wettability was determined by means of a modified capillary pressure method.

The application of silicones, up to a few equivalent monolayers, was found to be effective in altering the wettability of glass surfaces to a desired degree (up to contact angles of  $120^{\circ}$  as measured through the water phase). Although the application of HMDS changed the wettability of glass surfaces, its effectiveness could not be judged since small amounts of treatment could not be effected by means of the method used.

More studies are recommended for the perfection of techniques for the control of both packing and wettability.



## TABLE OF CONTENTS

### INTRODUCTION

### PART I

THEORY AND REVIEW OF LITERATURE	1
1. Geometries of Systematic Packing	1
2. Nature of Actual Packs	4
3. The Role of Vibration	7
4. The Mechanics of Vibrating Particles	11
5. The Influence of Different Variables	16
EXPERIMENTAL STUDIES	22
1. Design of Experiments	22
2. Experimental Studies	26
a. Preparation of Pack	26
b. Determination of Porosity	27
c. Determination of Permeability	27
d. General	29
RESULTS	31
1. Porosity Data	32
2. Permeability Data	43
CONCLUSIONS	45
NOMENCLATURE	47
BIBLIOGRAPHY	
APPENDICES	



## PART II

THEORY AND LITERATURE REVIEW	1
A. Wettability and Surface Forces	1
B. Nature of Glass Surfaces	7
C. Measurements of Wettability	12
EXPERIMENTAL STUDIES	18
1. Wettability Determination	18
A. Design of Experiments	18
B. Apparatus	20
C. Experimental Procedure	22
D. Description of Materials Used	25
2. Treatment of Glass Beads to Alter Their Wettability	27
A. Cleaning	27
B. Treatment with Silicone Fluid	27
C. Treatment with Hexamethyl-disilazane	28
3. Measurement of Other Properties	30
RESULTS	31
RECOMMENDATIONS	42
CONCLUSIONS	43
NOMENCLATURE	45
BIBLIOGRAPHY	
APPENDICES	





## LIST OF TABLES

### PART I

1. Features of Different Modes of Systematic Packings	2
2. Properties of Particles Used	25A
3. Summary of Porosity Data	33

### APPENDICES

1. Determination of Sizes of Particles	Appendix 1
2. Calibration of Amplitude Adjustment	2
3. Determination of Porosities of Packs	3
4. Determination of Permeabilities of Packs	3

### PART II

1. Effect of Silicone Treatment Upon Wetting Properties	32
2. Effect of HMDS Treatment Upon Wetting Properties	35
3. Effect of Silicone Treatment on Contact Angles Over Glass Surfaces	38



PART II CONTINUED

APPENDICES

1. Effect of Duration of Heating on  
the Reaction of HMDS with Glass  
Surface

Appendix 2

2. Determination of Contact Angles of  
Silicone and HMDS Treated Beads

3



## LIST OF FIGURES

### PART I

1. Design Of Cell and Accessories	24
2. Effect of Amplitude of Vibrations on Porosity of Packs of Different Types of Particles	35
3. Effect of Amplitude of Vibrations on the Condition Number of Packs for Different Particles	37
4.-8. Effect of Amplitude of Vibrations on Porosity of Different Individual Particles	Appendix 3

### PART II

1. Adhesion Tension and Contact Angle	2
2. The Mean Pore Radius in Case of Assemblages of Spheres	14
3. Flow Diagram for Capillary Pressure Measurements	21
4. Capillary Pressure Cell	24
5. Effect of Silicone Treatment on Contact Angles	33
6. Effect of HMDS Treatment on Contact Angles	36
7. Effect of Duration of Heating on the Reaction of HMDS with Glass Surface	Appendix 2



## INTRODUCTION

Investigators in many fields, especially Petroleum Engineering, use packed models to simulate natural porous media in laboratory studies. The materials involved are generally granular and non-cohesive in nature. The need to obtain a reproducible packed model, of desired bulk and flow properties, which would retain its properties during experiments is strongly felt.

The most important properties to control are porosity, permeability and wettability.

Mostly the methods of packing have been rather crude, utilizing many variations of shaking, tamping and compressing the models. Attempts in somewhat different directions have been made in the fields of ceramics and soil sciences, where mechanical vibrators were used for packing models. As yet, no satisfactory technique is available even for the case of uniform, spherical and non-cohesive particles.

The object of Part I of the present investigations was to study the nature of models packed with the use of a mechanical vibrator. The effects of different amplitudes of vibrations upon porosity and permeability of packs of Ottawa sand and glass beads of different types and sizes were studied.

It is expected that the information obtained from these studies may contribute towards better understanding and hence the evolution and standardization of







a satisfactory packing technique.

Recognizing the importance of wettability as is manifest by its influence on the fluid distribution, saturation, relative permeability and hence the entire phenomenon of flow and recovery of fluids; it becomes highly desirable that the two systems (Natural and the Packed model) should have identical wetting conditions.

The object of Part II of the investigations was to devise ways to alter the wettability of glass surfaces to desired extents.

Clean glass surfaces are known to be water wet. Effects of treatments of different amounts of Dow Corning 550 Silicone fluid and hexamethyldisilazane on the wettability conditions of glass surfaces were studied.

The contact angles were measured at atmospheric conditions, by means of a modified capillary pressure technique using iso-octane and 7.5% sodium chloride solution as fluid phases.



PART I

SIMULATION OF POROSITY AND PERMEABILITY



## THEORY AND REVIEW OF LITERATURE

### 1. Geometries of Systematic Packings:-

A packing may be defined as an arrangement of solid particles in which each constituent member is supported and held in place in the earth's gravitational field by tangential contacts with its neighbours.

The average number of tangent neighbours around each particle of the packing is called the condition number. If, in a packing of spheres, a small portion of a body is capable of complete representation of the manner of packing and distributions of the voids throughout the body, we refer to the packing as systematic and to the small portion as a cell. The smallest possible cell for the packing is called a unit cell. The ratio between the volume occupied by the voids and the bulk volume of a pack is called the porosity ( $\Phi$ ).

Graton and Fraser (1) describe six different modes of systematic packing of spheres. The salient features are shown in Table 1. It may be realised that in reality there are only four distinct modes of systematic packing of spheres since case III and VI as well as case II and IV are different orientations of the same cells.

From Table 1 it may be noted that whereas cubic is the "loosest" mode of systematic packing ( $\Phi = 47.64\%$ ); rhombohedral is the "tightest" mode ( $\Phi = 25.95\%$ ).



Table 1

Features of Different Modes of Systematic Packing

Features of the cells	Case 1	Case 2	Case 3	Case 4	Case 5	Case 6
Name (Crystal Analogy)	Cubic	Orthorhombic	Rhombohedral	Orthorhombic	Tetragonal Sphenoidal	Rhombohedral
Spacing of layers	$R\sqrt{4}$	$R\sqrt{3}$	$R\sqrt{2}$	$R\sqrt{4}$	$R\sqrt{3}$	$2R\sqrt{2/3}$
Condition Number	6	8	12	8	10	12
Face	90°	90°	90°	90°	60-120°	60° - 120°
Angles		60 - 120°	60 - 120°	60 - 120°	75°31' - 104°29'	
Interface	90°	90°	54°44' -	90°	90°	70°32' - 109°28'
Angles		60° - 120°	125°16'	60° - 120°	63°26' - 116°34'	
Porosity (%)	47.64	39.54	25.95	39.54	30.19	25.95







In the following discussion the term particle has been used to describe a spherical or nearly-spherical body.



## 2. NATURE OF ACTUAL PACKINGS

Considering porosity as a criterion for describing packings, it is observed that between two extreme cases of systematic packings - cubic ( $\phi = 47.64\%$ ) and the rhombohedral ( $\phi = 25.95\%$ ), there is an infinitude of unsystematic intermediate types, which may be termed "chance packings". These chance packings assume different geometrical configurations and porosities.

Systematic packing of a large number of particles in the laboratory requires a high degree of perfection in placement of different individual members. When a large number of particles is to be packed, this perfection is very unlikely to be attained. Instead, the required perfection would be confined to some rather limited portion of the packing, beyond which distortion of the array and "bridging" would begin, resulting in a chance, random or chaotic packing(2). Bridging causes an increase in porosity, and sometimes, as a result, a value of porosity greater than the of cubic packing is possible.

Random packs are known to assume porosities between 37% and 39%(3) and are often very unstable. Smith et al(4) report a linear relationship between the average condition number (N) of a random pack and its porosity ( $\phi$ ). They plotted a distribution curve



of the frequency of occurrence of particles with a particular condition number in a random pack, as a function of that condition number, and note that for random packs with mean porosities between 37% to 39%, these curves resemble Gaussian distribution curves. Furthermore, a pronounced shift in the peak of the distribution curve, toward larger condition numbers occurs as the overall porosity of the pack is decreased. Smith et al rule out the possibility of "bridging" occurring over an extended volume in random packings.

The particles in a pack are held in equilibrium by the interacting forces of gravity and by the normal and tangential components of friction. The pressure or overlying weight applied on the packs modifies the areas of contact between particles and hence the frictional forces.

Terzaghi (5) explains the phenomenon of settling of particles under the force of gravitation. When the falling particles touch the already settled particles, they rebound a little as a consequence of the reaction against penetration. The downward force of gravity and the upward reaction against penetration act as a couple to roll the particle till it reaches a depression. A very small intergranular bond (due to friction or overlying weight) is sufficient to overcome the tendency of the particle to overturn. Consequently it tends





to remain where it first fell. It is also recognized that since a particle in the interior can not change its position by passing between its neighbours without disturbing them (since considerable energy is required) it will tend to remain in the same neighbourhood. For the case in which the particles are packed in a rather limited space, Graton et al (6) pointed out that the effect of the boundary [due to discontinuity of the walls of the container] may not always be negligible. McGeary (7), after a mathematical analysis, concluded that if the ratio of diameter of container to diameter of particles is more than 10:1, the effect of the boundary is no longer felt.





3.

THE ROLE OF VIBRATION

The phenomenon of "bridging" occurs due to self-locking action of friction at the contacts between particles. It is realized that any type of moderate agitation - tamping, jarring, shaking or mechanical vibration may dislodge some of the relatively unstable particles and cause some type of restrictive flow, since dynamic friction is far less than static friction. This would move them to more stable positions with greater condition numbers and thus cause a more compact array. Vibrations are preferred since they provide more precisely controllable alternating stresses. Vibratory forces repeatedly increase and decrease the contact pressures between particles. Progressive slippage may occur due to the effect of such fluctuating pressures.

Mechanical vibration excites the particles to different levels depending upon amplitude and frequency of vibration and the elastic nature of the particles. Slade (8) suggests that a vibrating particle may be in one of three states of excitation:

- 1) A High Energy state in which the particles move sufficiently to bring about changes in the statistical characteristic of the medium, such as bulk density, porosity and permeability.

- 2) A Medium Energy State in which the partic-



ulate configuration of the medium undergoes irreversible local changes due to slipping, rolling or drifting of particles, without resulting in significant changes in the statistical characteristics of the medium.

3) A Low Energy State in which the changes in particulate configuration are cyclic.

Assuming the spheres to be sufficiently smooth and particles to be elastic, Hertz (as reported by Deresiewics(9)) has developed a theory of contact. When two spheres, each of radius  $R$ , are compressed statically by a force  $W$ , which is directed along their line of centres, the spheres contact each other on a circle of radius  $a_c$ , which is given by

$$a_c = (\theta WR)^{1/3} \quad (1)$$

where

$$\theta = \frac{3(1 - \sigma^2)}{4E}$$

$\sigma$  = Poisson's ratio

$E$  = Young's modulus

The normal pressure on the contact area is given by

$$P_m = \frac{3W}{2\pi a_c^3} (a_c^2 - \rho^2)^{1/2} \quad (2)$$

where  $\rho$  is the radial distance from the centre of the contact circle.

Actually contact occurs through surface asperities. In addition to the normal force  $W$ , other stresses such as shear, acting obliquely or tangentially, are imposed due



to overlying weight and reaction of friction at the contacts. When particles are in a state of vibration, the individual contact surfaces are subjected to forces whose normal as well as tangential components change simultaneously. In addition many local forces develop which in general are directed obliquely at the contact surfaces. Twisting couples might be present at many of these contacts. The presence of these, in addition to normal contact forces gives rise to force-displacement relationships which may be very complex and even in-elastic. Little work has been done in the direction of explaining the effect of vibrations in terms of normal forces and the coefficient of friction, which might explain geometric distortion of arrays due to vibration.

A particle under a high energy state of excitation, dislodged from its original location in the pack, would move around in the available space, in a slightly modified configuration caused by vibrations. The degree of freedom of movement of the particles would be gradually curtailed as the particle enters a position where it contacts more of the neighbouring particles. The contact with more neighbouring particles increases the friction and the particle loses all its freedom of movement in this position. It vibrates with its neighbours like a rigid body. It can still,





however, be dislodged from its new position, if a higher level of excitation, high enough to overcome static friction associated with particle, may be provided.

The configuration, while coming to rest, would exhibit a higher condition number and a lower porosity.

As has been already mentioned, Smith et al (10) report a linear relationship to be present between mean condition number and porosity for random packs. They point out that cubic packing ( $\Phi = 47.64\%$ ,  $N = 6$ ) and rhombohedral packing ( $\Phi = 25.95\%$ ,  $N = 12$ ) conform to the linear relationship, whereas tetragonal sphenoidal packings ( $N = 10$ ,  $\Phi = 30.19\%$ ) do not. Although special theoretical significance should not be attached to their proposed relationship, the average condition number calculated there-from, may serve as a rough index of porosity as well as frictional forces existing in the pack.

Deresiewicz (11), assuming that random packing was made up of, in part cubic and in part rhombohedral arrays, arrived at the following relationship between mean condition number and porosity.

$$N = 26.4858 - 10.7262/(1 - \Phi) \quad (3)$$

This relationship is based on the same concepts as described above.





#### 4. THE MECHANICS OF VIBRATING PARTICLES

A rigid body under vibration may have as many as six degrees of freedom. An assemblage of cohesionless particles does not act as a single rigid body but rather as a multiple mass system. Granular assemblages are reported to act as elastic bodies under repeated loading conditions (12, 13). The actual nature of vibrations may be very complicated but we may consider a rather simplified case of a particle under alternating vertical stresses, resulting in a simple harmonic motion of the type

$$x = a \sin wt. \quad (4)$$

where  $x$  is the displacement at any instant  $t$ ,  $w$  is the angular velocity, and  $a$  is the peak displacement from the mean position (or the amplitude). The acceleration acting will be given by

$$\frac{d^2x}{dt^2} = -a w^2 \sin wt. \quad (5)$$

Every elastic body has a natural frequency of oscillation  $f_0$  which may be expressed as

$$f_0 = \frac{w_0}{2\pi} = \frac{1}{2\pi} \sqrt{\frac{K_s}{M}} \quad (6)$$

where  $K_s$  is the equivalent spring constant and  $M$  is the mass of the vibrating body.

Damping forces are invariably present in any case of vibration. Their effect is to progressively decrease



the amplitude (in the case of free vibration\*) and to modify the frequency. This effect may be expressed in this form

$$W_d = 2\pi f_d = \sqrt{\frac{K}{M} - \frac{C^2}{4M^2}} \quad (7)$$

In this expression C represents the damping constant which, for a particulate body depends upon a great variety of variables and is best determined experimentally. It has been pointed out that in the determination of natural frequencies of particulate bodies, damping factors, if neglected, cause an error of the order of 2% (14, 15). The equivalent spring constant  $K_s$  may be defined as the force of movement required by a system to be displaced through a unit distance or rotated through a unit angle from its equilibrium position. Barkan (1934) [as reported by Tschebotarioff (16)] suggests that

$$K_s = \frac{pd}{S_e} \quad (8)$$

where  $pd$  is the alternating component of the average vertical contact pressure on the system due to dynamic forces and  $S_e$  is the elastic rebound determined by

---

\* Free vibrations are caused by the application of a single impulse (disturbing force), whereas forced vibrations are caused by periodic application of impulses.



static load test. Converse (17) suggests a semi-empirical approach and for his system he arrives at the relationship

$$K_s = 44.3 Mg + 1600 - 27F \quad (9)$$

where  $Mg$  is the dead load of the system and  $F$  is the dynamic force. It is recognised that the more compact and less compressible the system, the greater is  $K_s$ . The stress history influences the equivalent spring constant and the natural frequency, both of which may be changing under vibration. Tschebotarioff (18) has suggested that there is no such thing as a definite value for the natural frequency and states that instead, a determination of the range of natural frequencies may be more meaningful. For sand grains, these ranges lie in the interval of 1145 to 1685 cycles per minute.

When a system having a natural frequency  $w_o$  is vibrated at a frequency  $w_1$ , the amplitude of vibration is magnified by a factor  $\sum$  which is given by

$$\sum = \frac{1}{\sqrt{\left[1 - \frac{w_1^2}{w_o^2}\right]^2 - \left(\frac{2C}{w_o}\right)^2 \left(\frac{w_1}{w_o}\right)^2}} \quad (10)$$

The magnification factor  $\sum$  is greatest at the point where

$$w_1 = w_o \sqrt{1 - \frac{1}{2} \left(\frac{2C}{w_o}\right)^2} \quad (10a)$$

[It may be noted that if  $C = 0$ ;  $w_1 = w_o$ ]





This point is referred to as resonance. The exact resonant frequency is very difficult to predict due to the complicated nature of the assemblages. Experience in soil dynamics as well as in laboratory tests as reported by Converse et al (19) suggests that maximum compaction takes place at the resonant frequency.

The amplitude at resonance condition is given by

$$\begin{aligned}
 a_{\max} &= \frac{a}{\frac{2C}{W_0} \sqrt{1 - \frac{1}{4} \left( \frac{2C}{W_0} \right)^2}} & (11) \\
 &= \frac{a W_0}{2C} \left[ \text{since } C \ll W_0 \right]
 \end{aligned}$$

Beyond the resonant frequency, the peak amplitude decreases less rapidly with frequency as compared to its rate of increase below the resonant frequency (20).

A multiple mass system [viz. - vibrator - container - sample - load system] may have different resonant frequencies for different members and depending upon the interaction of amplitudes, there will be an optimum resonant condition with respect to any particular body. This makes the analysis of an actual system quite complicated.

If the vibrator is operated at resonant frequencies





of the laboratory building, foundation or that of the vibrator-container system, a structural damage may possibly occur as a result of surging stresses. Otherwise also, the inconvenience caused to the personnel make operation of vibrator at these frequencies very much undesirable. For utilising reasonably large magnification factors, operations should be conducted at a frequency larger than both these frequencies.



## 5. THE INFLUENCE OF DIFFERENT VARIABLES.

Since one of the main phenomena occurring during vibration is the relocation of particles to more favourable positions, it is obvious that a combination of vertical and horizontal amplitudes may prove more efficient than either. Very small amplitudes, of the order of 0.002", are comparatively ineffective. Winterkorn (21) suggests that the acceleration imparted to the particles is very important in governing their movement in the surface layers, while at depths, the amplitude of vibration plays the governing role. According to him, for maximum compaction the amplitude and the size of the particle to be moved should be of the same order of magnitude. Much larger amplitudes will cause shear, with concomitant loosening, and will result in an increase in porosity of the surface layers. It should be possible for a suitable load environment to inhibit this phenomenon.

In actual practice, grain surfaces are not microscopically smooth but have numerous asperities through which they contact each other. This roughness offers some frictional resistance which is proportional to the normal pressure applied, irrespective of wetness or dryness of the surfaces. Bowden and Tabor (22) point out that from Hertzian analysis (equations 1 and 2) the



area of contact is proportional to  $W^{2/3}$  and that mean pressure ( $P_m$ ) is proportional to  $W^{1/3}$ , where  $W$  is the normal force (applied) at the contacts. In the region of the particle, where the shear stresses are maximum, mean pressure  $P_m$  increases with the force  $W$  until the elastic limit of the material of particles is approached. Hertzian analysis also shows that this region is located at a distance of  $0.6a_c$  from the centre of the circle of contact. The elastic limit in this region is just exceeded when  $p_m = 1.11Y$  [where  $Y$  is the elastic limit of the material, as obtained in frictionless compression experiments.] This region yields plastically (partly irreversibly) while the rest of the particle still deforms elastically. Consequently, upon removal of stresses, only a slight amount of residual deformation remains. From the values of mean pressure  $P_m$  between  $1.11Y$  to  $3Y$ , the region discussed above flows plastically, increasing the size of the deformed area. Winterkorn (23) suggests that relocation of particles under vibration, when the applied static load is large enough to cause plastic flow, results in much more compaction than that achieved under a state of loading within elastic limits.

Johnson (24) suggests that for small tangential forces, the tangential displacement necessary to relieve obstruction in traction takes the form of an elastic





deformation of the asperities. The damage to the surface in this case is small and energy loss is largely due to elastic hysteresis. Hertzian analysis suggests that the energy loss should be proportional to the cube of the amplitude. However, for small amplitudes, the loss is found to be proportional to the square of amplitude rather than the cube (25). An increase in applied tangential force causes the asperities at the edge of the contact surface to deform plastically through relatively larger strains, which leads to a marked increase in energy dissipation and causes severe damage (fretting) to the surface. Finally near the values of tangential force sufficient to cause sliding, there is reasonable agreement between actual energy loss and that predicted by Hertzian analysis. Under such conditions, the vibrational movement at the contacts was found to have a self-cleaning action which might have broken down surface contaminant films (if any) and enabled the formation of local "cold-welded" junctions (26).

Very large stresses cause an increase in the area of real contact, thus aiding the "clamping" together of particles. This restricts relative tangential displacement of the particles and hence their relocation.

Since in the actual case of vibration of particles, the normal as well as tangential components of stress





change simultaneously, the stress-displacement relationship is guided not only by the instantaneous state of loading but by the entire loading history (27). Natarajan et al (28) suggest that there is an optimum static load for a given frequency, which yields maximum compaction. This optimum load depends upon the elastic properties of the particles and the moisture or lubricating conditions. They suggest that if the static load is added in increments up to the optimum load, while the pack is being vibrated, the greatest compaction results. It may be recalled that equation 9 suggests that the resonant frequency is influenced both by static load and dynamic force. The natural frequency of an assemblage of particles would thus be changing during the suggested cycle of operations.

Fatt(29) has investigated the effect of confining pressure on neoprene and steel spheres and for his system he arrives at the expressions, for neoprene spheres

$$V_{\text{void}} = 1560 - 60.5 P^{2/3} \quad (12a)$$

and for steel spheres,

$$V_{\text{void}} = 1420 - 0.242 P^{2/3} \quad (12b)$$

where  $P$  is the confining pressure in psia and

$V_{\text{void}}$  is the volume of void in the assemblage used.

An increase in temperature would cause thermal



expansion of the particles and the containing fluids. If the bulk volume is to remain constant, the increased confining pressure would cause further reduction of porosity.

It is recognized that large stresses are required to cause a slip or shear between dry surfaces. Moisture, in the form of films often acts as a good lubricant, consequently all soil compaction techniques use varying amounts of moistures. In the case of compaction of cohesionless particles, numerous experimenters and reports point out that best compaction is obtained under inundated conditions. Natarajan et al (30) suggest that smaller moisture contents introduce some type of apparent cohesion which hinders rather than aids compacting forces, whereas 100% moisture content destroys any such apparent cohesion. Tschebotarioff (31) suggests that every submerged particle is acted upon by bouyancy. This decreases the effective stresses between the particles and hence also the shearing strength and resistance to loading.

The duration of vibration under a particular load should be sufficient for all readjustments of the particle assemblage - fluid system to a more stable form. Natarajan et al (32) suggest that two minutes is sufficient for all such readjustments to take place, whereas Nagraj (33) suggests an interval of four to five



minutes.

The effect on compaction of particle size does not seem to be fully understood as yet. Westman et al (34) obtained better compaction (lower  $\phi$ ) with larger grains of the same material. Tschebotarioff (35) suggests that probably larger particles offer lesser resistance to dynamic forces. Johnson (36) points out that [referring to Formulae (1)] the radius of contact area is dependent upon the radius of the particles. A larger contact area undergoes lesser energy loss during relative movements of particles which are restricted due to increased friction. He also suggests that slip is proportional to  $R^{-1/3}$ , where  $R$  is the radius of the particle, i.e. larger particle would be subjected to small amounts of slip.





## EXPERIMENTAL STUDIES

### 1. DESIGN OF EXPERIMENTS

After an extensive study of the literature, it was decided that the particles be packed under vibration , at 100% water saturation condition. The cell was to be so designed as to be capable of allowing flow studies to be conducted with it. It was considered desirable that with the cell under vibration , static loads be applied in stages on the pack and the cell should provide due scope for application of such loads.

In view of the statistical variations anticipated, the studies to determine appropriate static load and duration of vibration were abandoned and instead an arbitrary static load of 3000 gms in stages of 1500 gms each and a duration of vibrations of 15 minutes per stage was selected.

The vibrator used in the studies was a 20 inch square Syntron model VP60 vibrating table. The vibrator contained an electromagnetic assembly as the source of vibrations. The vibrator provided an adjustable switch to regulate the amount of current fed to the assembly and hence the amplitude of vibrations. A graduated circular scale with readings from 0 to 100, was fixed around the adjustable switch to help the regulation of amplitude. No device to control the frequency





of vibration was available with the vibrator used.

In order to ensure consistency of results, it was considered desirable that the cell be reproducibly placed at a particular spot on the vibrator table. A Y-shaped frame with a circular hub in the middle to hold the cell was used for securing a rigid connection between the cell and the vibrator table.

Since the applied load must cover the entire circular cross-section of the cell, and yet provide channels for water to be squeezed out (in order to facilitate compaction) a piston type hollow tube with rubber padding at the bottom was designed. A circular extension of the cell, to guide the movement of the piston was provided. Lead shot was chosen as the means for providing load. This choice permitted load schedule changes to be made with ease.

After studying the phenomenon of settling of particles, it was proposed that better results may be obtained if all the particles are introduced into the cell while it was vibrating. Cardboard funnels with a 2mm opening were provided to obtain a slow and roughly reproduceable rate of filling.

The final design of the cell is presented in figure 1. Meshes were fitted at the bottom of the cell and in the flow channel of the lid in order to retain the



particles within the cell during flow tests.

In order to avoid Bournoulli's effect, while determining pressure drop across the packs during flow tests, pressure taps were provided at the locations shown in the figure.

Four different sizes of glass beads and graded Ottawa sand were used in all packing studies. The properties of glass beads and the Ottawa sand are given in Table 2.



## 2. EXPERIMENTAL STUDIES

### a) Preparation Of Pack.

The cell was cleaned, assembled and the weight of the empty cell with its accessories was determined. Deaerated water was poured into the cell along a rod in order to prevent the introduction of air bubbles. The extension was then screwed into the cell; the cell-extension assembly mounted on the vibrator and the vibrator turned. Particles were then introduced into the cell through a cardboard funnel until the level of the particles reached a fixed mark within the cell. Vibration was permitted to continue for 15 minutes. At the end of this time the load-piston, containing sufficient lead shot so that the combined weight of piston and shot was 1500 gms, was inserted into the cell. Vibration was permitted to continue for another 15 minutes, at the end of which, an additional 1500 gms of lead shot was placed in the load-piston. Vibration was continued for another 15 minutes. Then the vibrator was switched off, the piston and extension removed and the weight of the packed particles was determined. The height measurement was obtained by placing a smooth cylindrical extension on the pack surface and measuring the elevation of the extension by means of a cathetometer. The lid was placed and locked in





TABLE 2

Sample No.	Designation	Material	Colour	Mean Dia.	Specific Gravity	No. of Observations
1	Small Beads	Soda-lime Glass	Transparent with greenish shade	0.01714 cm	2.4404	20
2	Medium Beads	Borosilicate glass	Transparent with yellowish shade	0.0518 cm	2.590	22
3	Big Beads	Borosilicate glass	Transparent with bluish shade	0.0989 cm	2.4404	29 (15*)
4	Ottawa Sand	Natural sand (quartz mostly)	Brown	0.0825 cm	2.6513	22 (18*)
5	Brown Beads	Borosilicate glass	Brown	0.0142	2.5620	20

\* (Permeability Readings)



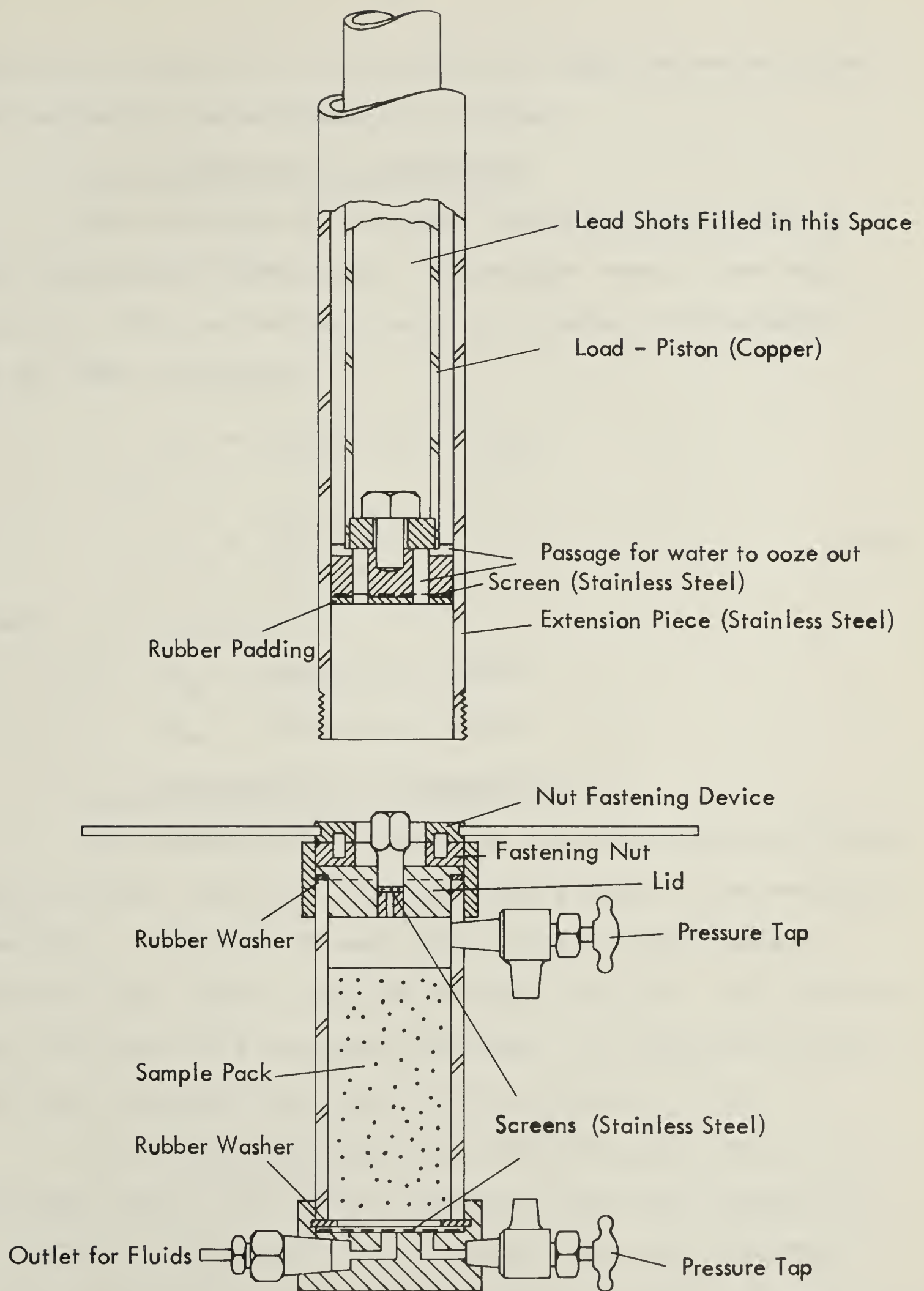


FIG. 1. DESIGN OF CELL AND ACCESSORIES



position by means of the fastening nut and the whole system was weighed to an accuracy of 0.01 gms.

#### b) Determination of Porosity

From the mass of the water saturated porous medium and its physical dimensions, its average density was calculated. This in turn was used to calculate the porosity of the pack as follows

$$\begin{aligned}\rho_a &= \rho_g (1 - \phi) + \rho_w \phi \\ \phi &= \frac{\rho_g - \rho_a}{\rho_g - \rho_w}\end{aligned}\tag{13}$$

where

$\rho_g$  = Density of glass

$\rho_w$  = Density of water

#### c) Determination of Permeability

The permeability of the pack was determined by flowing water through the pack, with the cell placed in the vertical position. Water was flowed from a constant head vessel, through tygon tubing and then through the pack. The effluent was collected in a graduated cylinder. The duration of the test was measured with the aid of an electric clock.

The pressure differential across the pack was measured using a  $\text{CCl}_4$ -water manometer which was mounted on a vertical panel board. The pressure taps were connected to the manometer by means of 1/4" copper tubing. In each case flow was initiated and approximately 100 pore volumes of fluid was allowed to pass prior to the





measurement of flow rate so as to permit stabilization. The flow rate was taken as the mean of three consecutive runs, which generally agreed within 0.02 minutes per 250 cc of throughput. The pressure drop  $\Delta P_w$  was calculated using the relationship

$$\Delta P_w = \Delta P_{\text{man}} \quad (14a)$$

where  $\Delta P_w$  = total effective pressure drop in terms of head of water.

$\Delta P_{\text{man}}$  = Pressure drop across the taps  
[in terms of head of water]

The permeability was calculated from Darcy's law as follows

$$q = - \frac{K}{\mu} A \frac{\Delta P_w}{L}$$

$$\text{or } K = \frac{-q\mu L \times 1033.6}{A\Delta P_w} \quad (14b)$$

where  $K$  = permeability [Darcy's]  
 $\mu$  = viscosity [centipoises]  
 $L$  = length of the pack [cm.]  
 $A$  = area of cross section of pack [square cm]  
 $1033.6$  = a unit conversion factor.

Upon completion of a series of tests the particles were placed in a china dish and washed with water and occasionally with chromic acid, then oven dried for about three hours and stored for re-use. They were





occasionally examined microscopically to check for strain, fretting or breaking.

d) General

The size of particles was measured using a travelling microscope and the mean of a number of different readings calculated and recorded as shown in Appendix 1.

The specific gravity of the particles and of  $\text{C Cl}_4$  was determined through the use of specific gravity bottles.

The frequency of the vibrator with cell mounted on it was measured with a stroboscope. The amplitude of vibration was determined by operating the stroboscope at a frequency, very close to that of the vibrator, so that there were very few beats. The span of a particular amplitude of vibration could thus be observed under virtual slow motion of the vibrator. The amplitudes were optically magnified by means of a lamp and scale arrangement.

The source of light in the stroboscope was covered with an opaque tape, leaving a small aperture so that it could behave like a point source and thus provide a sharp beam of light. This thin beam of light was reflected by a small mirror, mounted on the vibrator table, and its movement was observed on a piece of paper. The piece of paper was placed at some greater



distance from the light source. The extreme positions travelled by a particular point in the reflected beam were marked on the paper and measured with the help of a diagonal scale. The relationship between the amplitudes of vibrations (peak to peak) and the values of amplitude-setting was found to be linear. Appendix 2 gives details of the determination of this relationship.



## RESULTS

The observations taken for the determination of porosity and permeability of packs of different particles are presented in Tables 1 to 5 of the Appendix III.

Permeability data were taken on packs of Ottawa sand and Big beads only. Tables 6 and 7 of Appendix III present the details of calculation of permeability of the packs.

Periodic microscopic examination of particles revealed no broken or deformed particles. Probably as a consequence of fluctuating contact pressures and the sliding of glass beads over one another, several glass bead samples exhibited noticeable scratches.

The values of porosity, as calculated in Appendix 3, are plotted in figures 4 to 9 for different particles as a function of amplitudes of vibration. It may be observed that the same type of packs prepared under similar conditions of vibration show considerable scatter. For example, 5 different packs of Big beads, packed under identical conditions (peak to peak amplitude value 0.840 mm corresponding to setting 10.0 of the vibrator) show values of porosity as 33.25%, 32.96%, 33.90%, 33.92% and 33.70%. The scatter of observed values of permeability was much wider. The results are discussed under separate headings in the following sections.





## 1. POROSITY DATA

The observation of considerable scatter in the porosity data as plotted in Figures 4 to 8 necessitated the determination of a median line through the observation points in each of the above figures. The packs were prepared at different amplitudes of vibrations, ranging between 0.56 mm and 1.26 mm (peak to peak). Very little was known about the anticipated values of porosity of packs, prepared under an amplitude of vibration which was outside the above range. Under these conditions, for simplicity, a linear fit for the median line of the data was decided upon. Simultaneously it was considered desirable to obtain a straight line fit for the corresponding condition numbers.

The details of the fits desired, and the results obtained from a computer programme, together with values of standard deviations are presented in Appendix 3. A summary of equations of straight lines obtained from the computer analysis is presented in Table 3. For the range of amplitudes studies, these lines are plotted as solid lines in Figure 2. Figure 3 presents a similar plot of condition number (N) versus amplitudes of vibrations. In the representation of formulae of straight lines in Table 3, the symbol  $z_a$  is used to denote peak to peak amplitude in millimeters, so as to differentiate it from  $a$ , which represents the value of half the peak to peak amplitude.



TABLE 3

Equations of straight line fits of Amplitude - Property relationships  
for Different Samples

Designation of sample	Material	Mean dia. of particle	$\Phi$ - za relationship	N - za relationship	Standard Deviation
Big Beads	Borosilicate Glass	0.0989 cm	$\Phi = 35.284 - 2.6052a$	$N = 9.9273 + 0.6249 za$	0.414
Medium Beads	Borosilicate Glass	0.0518 cm	$\Phi = 37.407 - 2.607 za$	$N = 9.3699 + 0.6662 za$	0.398
Brown Beads	Borosilicate Glass	0.142 cm	$\Phi = 37.895 - 2.245 za$	$N = 9.2280 + 0.5880 za$	0.383
Small Beads	Annealed soda Lime Glass	0.172 cm	$\Phi = 37,116 - 2.388 za$	$N = 9.4432 + 0.6089 za$	0.328
Ottawa sand	Silica ( $\theta z$ )	0.0825 cm	$\Phi = 36.664 - 4.234 za$	$N = 9.5930 + 1.015 za$	0.281



Any discussion of amplitude of vibration brings into consideration the magnification factors due to interaction of natural and forced frequencies of vibration and hence, the evaluation of the natural frequency of vibration. In view of the complexities due to the number of degrees of freedom and involvement of different geometries and materials, such evaluation becomes very complex. For the experimental setup used, it may be expected that the value of natural frequency will be slightly increased due to interference with other vibrating bodies. In fact it may reach values as high as 1800 - 2000 rpm. The frequency of vibration of the system is 3775 rpm which is nearly twice the value of the natural frequencies of the samples. Since all samples are of the same composition and nature, the range of natural frequencies is expected to be small. Under these conditions, it seems that the magnification of the amplitudes of vibrations, due to interaction between natural and forced frequencies, was of a similar order for different test samples.

As can be observed from figure 3, in general lower values of porosity were recorded with higher values of amplitude. This supports the views expressed in the literature that progressive slippage occurs with higher and higher values of amplitude of vibration.





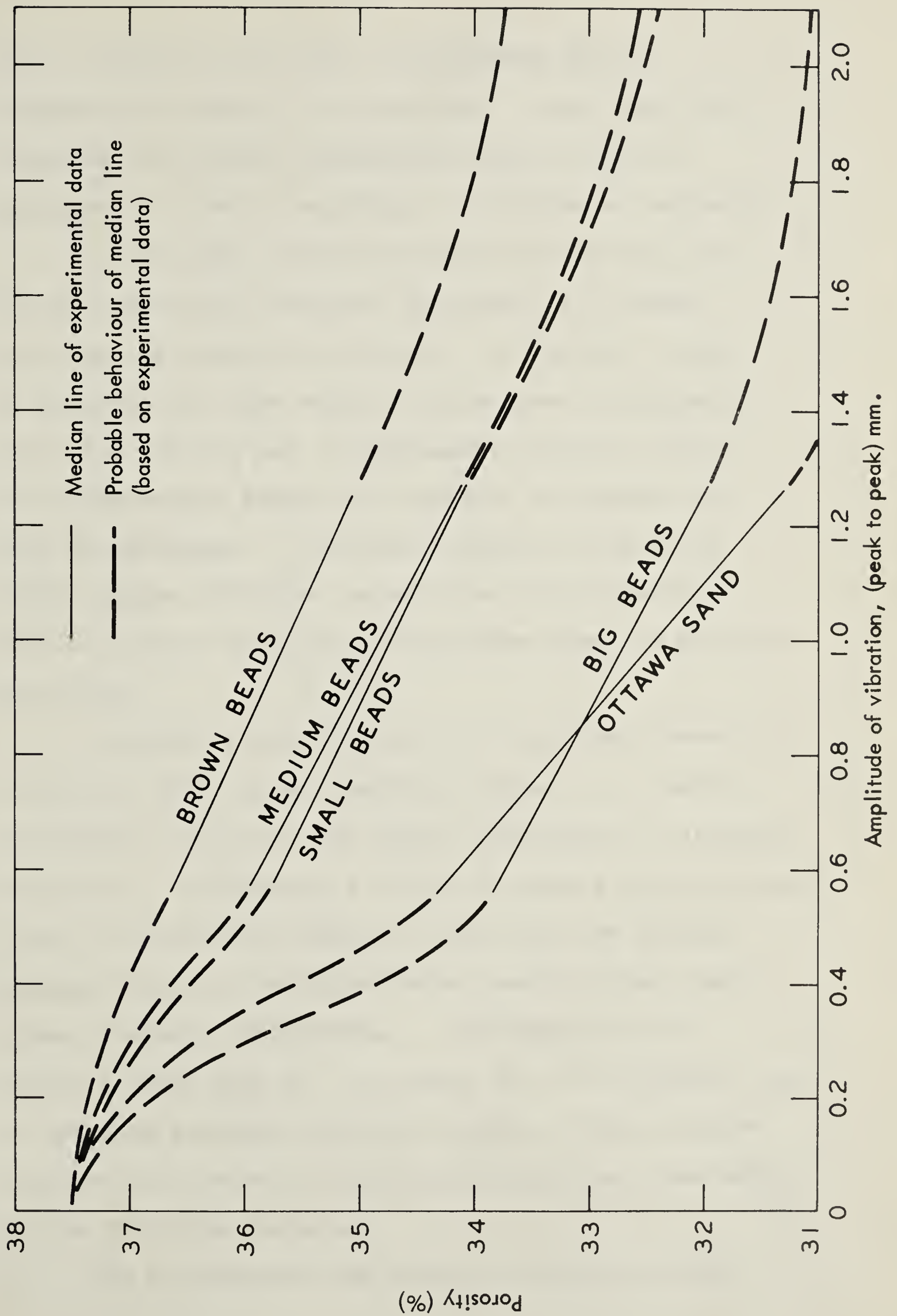


FIG. 2. EFFECT OF AMPLITUDE OF VIBRATIONS ON POROSITY OF PACKS OF DIFFERENT TYPES OF PARTICLES





Many a sphere in the pack is supported by the neighbouring spheres in a position other than that required for maximum compaction, due to high coefficient of static resistance to sliding at contacts.

It has been earlier pointed out that the condition numbers of different particles in a random pack exhibit normal distribution. Likewise, it may be expected that the contact resistances at different particles arising out of different condition numbers in a random pack should also exhibit a somewhat similar distribution. Different contact resistances would require different intensities of displacing forces during vibration to overcome them and relocate particles.

It seems probable that as the particle moves to a position with higher condition numbers, the number of contacts and hence the static resistance to slipping increases. Consequently it would require an even higher level of displacing forces to move from its current location. Thus the condition number seems to be a good index of static resistances. An examination of figure 3 shows that  $\phi - z_a$  curves for the different types of specimen followed different trends. This is to be expected in view of the different nature and dimensions of the particles involved.

It is observed from figure 3 that porosities



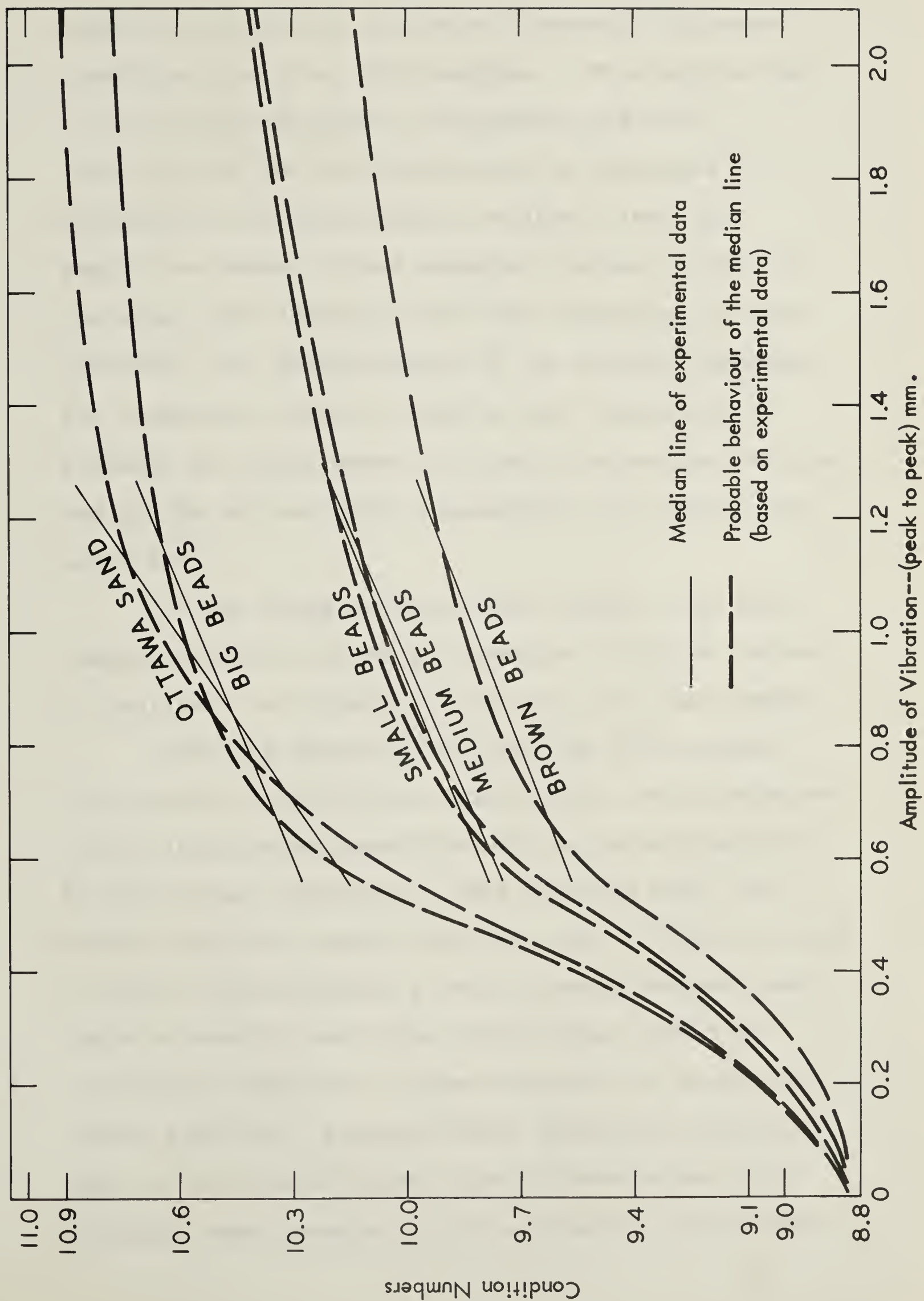


FIG. 3. EFFECT OF AMPLITUDE OF VIBRATIONS ON THE CONDITION NUMBERS OF PACKS FOR DIFFERENT PARTICLES





obtained with Ottawa sand show a somewhat different trend than the other four samples. This may be due to the surface roughness, angularity and non-sphericity of the sand particles, as indicated by microscopic and photographic studies. Since this sample has shown a trend somewhat similar to that of the other four samples, which were spherical or near spherical, the effectiveness of the present technique for compacting natural sands is also demonstrated. Probably the differences in elastic properties of glass and quartz may be partly responsible for some of the deviations.

In the range of amplitudes studies, the sand samples seemed to be more responsive to higher values of amplitude of vibration than were the glass beads.

From the observed data for the five samples, the diameter of particles seems to be a very important factor influencing porosities of the packs prepared by the present technique. Data obtained with Big, Medium and Brown beads, which are made of similar types of glass (borosilicates), very strongly suggest that packs of smaller particles yield higher values of porosity as compared to those obtained for packs of larger particles, prepared under identical conditions. Data for Small beads do not seem to corroborate this inference when compared to those from the above three





TABLE 4

Influence of Diameter of Particles Upon Porosities  
Observed under Vibration.

Material	Diameter mm	Porosity Ø%	Source
Washed sand	.711	38.2	Westman and Hugill (37)
Washed sand	.252	38.6	
Washed sand	.089	42.5	
Natural co- hesionless soil	.22	36.0	U.S. Waterways Station (38)
	.29	36.7	
	.30	35.5	
	.46	35.0	
	.60	29.6	
	1.0	29.6	



types of glass beads. This behaviour of Small beads may probably be ascribed to the differences in the elastic natures of small beads (soda-lime glass) and the other three types of beads (Borosilicate glass). Poor statistics may also be attributed to this difference.

Table 4 presents more data from the literature to support this inference regarding the influence of diameters on porosities of packs. No values of amplitudes or ranges thereof were specified in the sources of data of Table 4.

The influence of size of particles upon the resultant porosity may probably be explained in the following way. Johnson (39) has stated that slip is proportional to  $w^{2/3}/R^{1/3}$ . This means that larger particles should provide lesser slips as compared to smaller particles. Again, as is indicated by Hertz's theory (relation 1) the area of contact between two particles is proportional to  $R^{1/3}$ . This indicates that a bigger particle should overcome greater resistance for the same amount of slip.

It is common knowledge that the number of smaller particles occupying a certain bulk volume is much larger than the number of bigger particles occupying the same space. This requires more net frictional resistance per bulk volume to be overcome by smaller



particles as compared with that for larger particles. Under a particular amplitude of vibrations the assemblages of larger particles overcome larger net frictional resistance and hence provide lower porosity values.

Smith et al (40) report an average condition number of 8.84 for a random packing of spheres. McGeary (41) reports a random packing of spheres with a porosity of 37.5%; which is also the generally accepted value of porosity of random packing. It is realized that a value of zero amplitude of vibration will produce a random packing. Taking these figures as fixed for zero amplitudes of vibrations, and observing the trend of median lines of data in the amplitude range investigated, it is possible to intuitively suggest the probable behaviour of the median lines.

For very small values of amplitude of vibration, there is likely to be no movement (sliding or slipping) of particles until the displacing force attains a sufficient level to overcome the static resistance of the particles. Once a minimum value of amplitude is reached to cause displacement of a particle, successive increases would bring about more relocations of particles. At the same time, since the overall condition number will be increasing, the particles with greater condition numbers will also be





increasing in number. In this interval, the effect on porosity would be rather large and a steep trend would be observed. During this process, many particles would enter positions that would require very large displacing forces for relocation. In this way, with increasing amplitudes of vibration after a certain level, fewer particles would be relocated and the system would show a value which would be the minimum porosity obtainable by the technique for the sample, under a particular load environment. Dotted line curves are drawn on figures 2 and 3 according to this line of thinking, encompassing the observed data. More data obtained with different materials would promote better understanding of the phenomenon of packing under vibrations.





## 2. PERMEABILITY DATA

Appendix 3 presents the calculation of permeability values for packs of Ottawa sand and Big beads. The values of permeability of different packs show wide variations amongst themselves and lie between 130 to 390 darcies in the case of Ottawa sand and between 460 to 810 darcies in the case of Big beads.

The Carman-Kozeny relationship states that for packs of uniform spherical particles,

$$K = \frac{d^2 \phi^3}{180(1 - \phi)^2}$$

where

$K$  = permeability (sq.cm.)

$\phi$  = porosity (fraction

and  $d$  = diameter (cm.)

The values of permeability calculated using the above relationship and the observed values of permeability of different packs are in disagreement, by as much as 30% and 50%, and this discrepancy could not be explained. Probably air (or gases) occluded in the pack or brought in solution and released in the packs might have caused some errors. It is also possible that the discrepancy may be partly due to some over simplified assumptions in the derivation of the Carman-Kozeny relationship.

It is common knowledge that whereas porosity is a bulk property, permeability is a geometrical property,



which is very much dependent upon the geometrical distribution, shapes, sizes and orientation of different void spaces. With this in view, achieving a reproducibility in the values of permeability for different packs appears to be a more difficult operation than achieving it (reproducibility) in the values of porosity. Probably that is why the permeability values of the packs could not be correlated either with the porosity values or the amplitudes of vibrations.

The small autoclave 1/8" connections and tubes had to be cleaned many times as they showed a tendency to accumulate dirt, thereby offering additional resistance to flow. It may be pointed out that after each experiment, if the tubes showed any accumulation of dirt, the readings for permeability determination were discarded. Probably bigger fluid inlet and outlet connections may help in reducing the above disadvantage.

More work is needed to study the feasibility of attaining a reproducibility in the values of permeability of packs, within some reasonable range.



### CONCLUSIONS

1. A technique using vibrations is proposed for packing granular material, so as to reproducibly obtain any porosity within a reasonable range of deviations.
2. The porosity of packs obtained by the proposed technique is influenced, among many variables, by the elastic nature of the material ( $E, \sigma$ ), its diameter, shape and roughness, and the amplitude of vibrations.
3. Lower porosity values are obtained with higher amplitudes of vibrations, and for the range of amplitudes studied, there seems to be a linear relationship between porosities and amplitudes of vibrations.
4. Particles of larger diameter, when packed by the proposed technique, show lower values of porosities as compared to those shown by smaller diameter particles of the same material packed under identical conditions.
5. Permeabilities obtained from packs prepared by the above technique show too much variation and an improvement in the technique is required to obtain reproducible values of both porosity and permeability.





6. More investigation concerning the influence of different variables on porosities and permeabilities is required for perfecting and standardizing the technique.



NOMENCLATURE

A	Area of crossection of the cell (or pack) (square cm)
a	Amplitude of vibration (Millimeter)
ac	Radius of circle of contact between two elastic spheres (cm)
C	Damping constant of a vibrating body
d	Subscript for damped condition of vibration
E	Young's modulus of elasticity (gms/cm)
f	Frequency of vibration (cycles per second)
g	Acceleration due to gravity (cm/sec <sup>2</sup> )
K	Permeability (darcies)
K <sub>s</sub>	Spring constant
L	Length of Pack (cm)
L <sub>taps</sub>	Distance between the pressure taps (cm)
M	Mass (gms)
N	Condition Number
o	Subscript for undamped vibrating conditions
P	Pressure (gms/cm <sup>2</sup> )
P <sub>mean</sub>	Mean Pressure (gms/cm <sup>2</sup> )
pd	Alternating component of average vertical contact pressure on the system due to dynamic forces (gm/cm <sup>2</sup> )
R	Radius of spheres (cm)
Se	Elastic rebound (gms/cm <sup>2</sup> )
t	Time (seconds)
V <sub>voids</sub>	Volume of voids (cm <sup>3</sup> )



W	Normal force of contact (dynes)
w	Angular velocity (radians/sec)
x	Displacement (cm)
Y	Elastic limit of material (gm/cm <sup>2</sup> )
za	Peak to peak amplitude of vibration (mm)
Δ	Difference
θ	A constant elastic property (gms/cm <sup>2</sup> ) $= \frac{3(1 - \sigma^2)}{4E}$
μ	Viscosity (centipoise)
ρ	Radial distance between circumference of the circle and centre of contact (cm)
ρ	Density (gms/cm <sup>3</sup> )
ρ <sub>a</sub>	Apparent density of pack (gm/cm <sup>3</sup> )
ρ <sub>g</sub>	Density of glass (gm/cm <sup>3</sup> )
ρ <sub>w</sub>	Density of water (gm/cm <sup>3</sup> )
Σ	Magnification factor for amplitude
σ	Poisson's Ratio
Φ	Porosity (fraction or %)





## BIBLIOGRAPHY

1. Graton, L.C. and Fraser, H.J.  
     "Systematic Packing of Spheres"  
         Jour. of Geology Vol. XLIII (1935)  
         No. 8, Part I, pp 785-909
2. Muskat, M.  
     "The Flow of Fluids Through Porous Media"  
         McGraw-Hills, New York, 1937, page 12
3. Westman, A.E.R. and Hugill, H.R.  
     "The Packing of Particles"  
         Jour. Am. Cer. Soc. Vol. 13 (1930)  
         pp 767-779
4. Smith, W.O.; Foote, P.D. and Busang, P.F.  
     "Packing of Homogeneous Spheres"  
         Physical Review Series 2, Vol 34 (1929)  
         pp 1271-74
5. Terzaghi, K.  
     "Modern Concepts in Foundation Engineering"  
         Jour. Boston Soc. of Civil Eng. Vol. XII (1925)  
         pp 397-402
6. Graton, L.C. and Fraser, H.J. - op cit.
7. McGeary, R.K.  
     "Mechanical Packing of Spherical Particles"  
         Jour. Am. Cer. Soc. Vol. 44 (1961)  
         pp 513-522
8. Slade, J.J. (jr.)  
     "A Discontinuous Model for the Problem of  
         Soil Dynamics"  
         Symposium on Dynamic Testing of Soils,  
         A.S.T.M. Special Tech. Pub. No. 156 (1953)
9. Deresiewicz, H.  
     "Mechanics of Granular Matter"  
         Advances in Applied Mechanics, Vol. 5 (1958)  
         A.P. New York



BIBLIOGRAPHY

10. Smith et al - op cit
11. Deresiewicz, H. - op cit
12. Terzaghi, K.  
    "Theoretical Soil Mechanics"  
        Chapter XIX, Wiley, New York (1943)  
        pp 434-479
13. Tschebotarioff, G.P.  
    "Soil Mechanics, Foundations and Earth  
        Structures"  
        McGraw-Hill (1951) , Chapter XVIII  
        pp 568-595
14. Converse, F.J.  
    "Compaction of Sand at Resonant Frequency"  
        A.S.T.M. Special Tech. Pub. 156 (1953)  
        pp 124-137
15. Pauw, A.  
    "A Dynamic Analogy for Foundation - Soil Systems"  
        ibid pp 90-112
16. Tschebotarioff, G.P. - op cit
17. Converse, F.J. - loc. cit.
18. Tschebotarioff, G.P. - op cit
19. Converse, F.J. - op cit
20. Terzaghi, K. - op cit (same as 12)
21. Winterborn, H.F.  
    "Macromeritic Liquid"  
        S.T.P. 156 (1953) pp 77-89
22. Bowden, F.P. and Tabor, D.  
    "The Friction and Boundary Lubrication  
        of Solids"  
        Oxford (1950)



## BIBLIOGRAPHY

23. Winterkorn, H.F. - op cit
24. Johnson, K.L.  
     "Surface Interaction Between Elastically  
     Loaded Bodies Under Tangential Forces"  
     Proc. Royal Soc. (London) Series A  
     Vol. 230 (1955) pp 531-548
25. Deresiewicz, H. - op cit
26. Johnson, K.L. - op cit
27. Deresiewicz, H. - op cit
28. Natarajan, T.K. and Palit, R.M.  
     "Combination of Static and Dynamic Load  
     Effects for the Compaction of Cohesionless  
     Soils".  
     Int. Soc. of Soil Mech. & Found. Eng.  
     Regional Conf. (ASIA), New Delhi, Feb.  
     1960.
29. Fatt, I.  
     "Compressibility of a Sphere Pack - Comparison  
     of Theory and Experiment"  
     Jour. of App. Mech. Vol. 24 March 1957,  
     pp 148-;49
30. Natarajan et al - op cit
31. Tschebotarioff, G.P. - loc cit
32. Natarajan et al - op cit
33. Nagaraj, C.N.  
     "Effect of Vibration on Settlement"  
     Symp. on Found. Eng. Indian National Soc. of  
     Soil Mech and Found. Engg., New Delhi,  
     Jan. 1961.
34. Westman et al - op cit



## BIBLIOGRAPHY

- 35. Tschebotarioff, G.P. - op cit
- 36. Johnson, K.L. - op cit
- 37. Westman et al - op cit
- 38. U.S. Waterways Experimental Station, Vicksburg (Miss,) "Soil Compaction Investigation Report No. 5"  
Tech. Mem. No. 3 - 271 June 1950
- 39. Johnson, K.L. - op cit
- 40. Smith et al - op cit
- 41. McGeary, R.K. - op cit





## APPENDICES



APPENDIX 1DETERMINATION OF MISCELLANEOUS PROPERTIES.

1. SIZE OF THE PARTICLES:- Using a travelling microscope, the size of a number of different particles was measured as shown in Table I.

TABLE IDETERMINATION OF MEAN DIAMETERS OF PARTICLES

(all measurements in centimeters)

Type of Beads	Ottawa Sand	Big Beads	Medium Beads	Small Beads	Brown Beads
Measurements	.076	.099	.047	.024	.014
	.080	.104	.053	.018	.016
	.092	.083	.051	.019	.015
	.078	.088	.056	.016	.015
	.071	.091	.054	.012	.013
Mean	.0825	.0989	.0518	.0171	.0142

2. SPECIFIC GRAVITIES OF DIFFERENT PARTICLES AND  $\text{CCl}_4$ :

The specific gravities of different particles, as measured through the use of a relative density bottle is as follows:



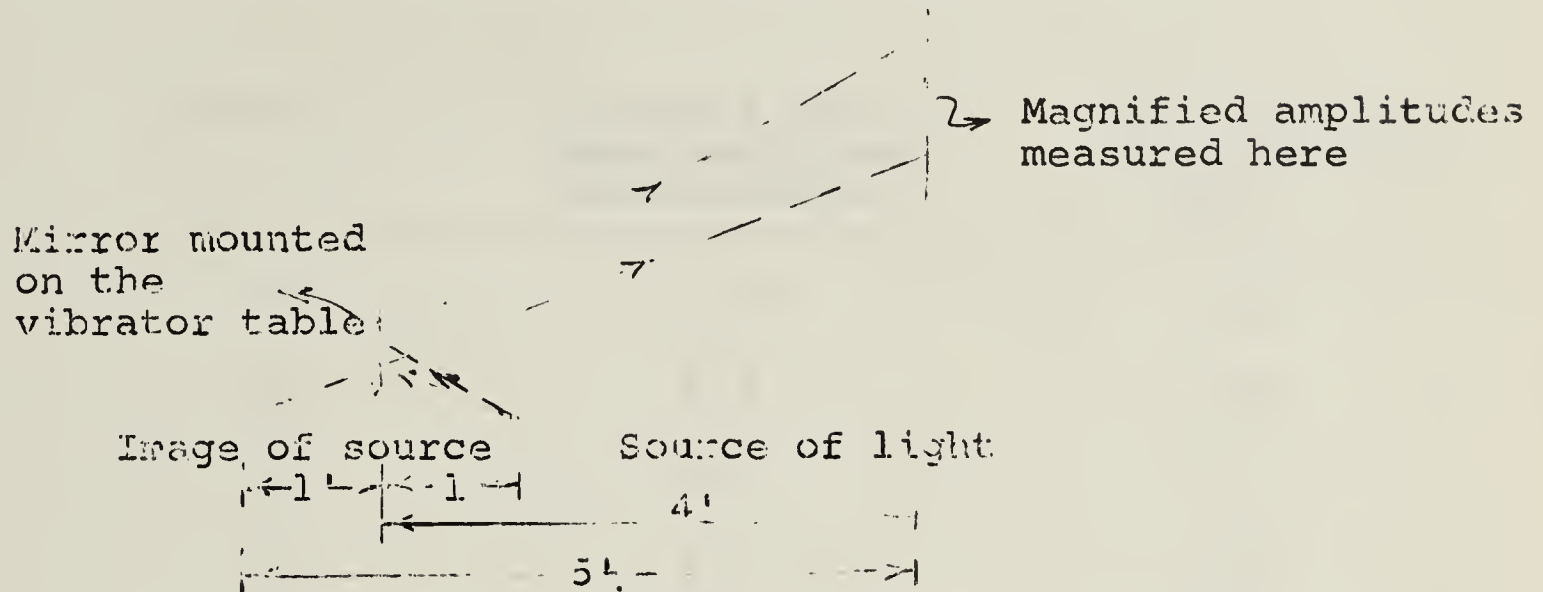
<u>Sample</u>	<u>Specific Gravity</u>
Big Beads	2.441
Medium Beads	2.590
Small beads	2.441
Brown Beads	2.561
Ottawa Sand	2.651
CCl <sub>4</sub>	1.587

3. DETAILS OF THE CELL:

Constant weight	=	3430.190 gms
Diameter	=	5.058 cm.
Area of crossection	=	20.1488 sq. cm
Height from mesh to cap=		16.250 cm





APPENDIX 2CALIBRATION OF AMPLITUDE SETTING OF THE VIBRATOR:-

The positions of stroboscope light source, mirror mounted on vibrator table and of observation paper are shown in Figure 9. Following observations were made:

Frequency of vibration = 3770 cycles/minute

Magnification factor = 5

The measurements for determination of amplitudes are shown in Table 1.



TABLE 1

Setting	Observed Peak to Peak Amplitude (millimeters)	Actual peak to peak amplitude (za)
30	7.02	1.40
25	6.4	1.28
20	5.6	1.12
15	4.9	0.98
10	4.2	0.84
5	3.5	0.70
Omax	2.8	0.56

From the above the following equation of a straight line was derived:

$$za = 0.56 + 0.028 {}^a\text{set} \left[ \text{millimeter} \right]$$

where  ${}^a\text{set}$  is the scale reading of amplitude adjustment on vibrator.



APPENDIX III

A) Calculation of Porosity: - The porosity of the prepared packs of beads was determined by noting the weight of cell and its content and the height of a measuring extension piece projecting over the upper edge of the cell, when the piece is placed on the pack. A sample calculation is show below -

A pack of Ottawa beads(Sp gr.,2.6513) prepared using an amplitude setting of 10, weighed 3949.65 gms and the height of an extension piece projecting out was 0.895cm. The empty cell, with all accessories, weighed 3430.19gms. The height of top of cell from bottom mesh was 16.25cms and the distance between bottom of the cap and the top of the cell is 3.20cms. The area of crossection of cell was 20.1488 sq. cm. From the above data, we obtain,

$$\begin{aligned} \text{Length of the pack} &= 16.25 - 5.70 + 0.895 \\ &= 11.445 \text{ cm} \end{aligned}$$

$$\begin{aligned} \text{Volume of Pack} &= 11.445 \times 20.1488 \\ &= 230.60 \text{ c.c.} \end{aligned}$$

$$\begin{aligned} \text{The space between the top of the pack and cap} &= 16.25 - 3.20 - 11.445 \\ &= 1.605 \text{ cm} \end{aligned}$$



$$\begin{aligned}
\text{Volume of space filled with water} &= 1.605 \times 20.149 \\
&= 32.24 \text{ c.c.} \\
\text{Weight of this volume of water} &= 32.24 \text{ gms} \\
\text{The weight of the contents of cell} &= 3949.65 - 3430.19 \text{ gms} \\
&= 519.46 \text{ gms} \\
\text{The weight of the pack} &= 519.46 - 32.24 \text{ gms} \\
&= 487.22 \text{ gm} \\
\text{Apparant Density of Pack} &= 487.22/230.60 \\
&= 2.1128 \text{ gms/c.c.} \\
\text{The porosity of the pack} &= \frac{\rho_a - \rho_w}{\rho_g - \rho_w} \\
&= \frac{2.1128 - 1.0}{2.6513 - 1.0} \\
&= \underline{32.61\%}
\end{aligned}$$

The observations are shown in the first three columns of Tables 1 to 5 for different particles, figures 4 to 9 show the porosities thus obtained, as functions of amplitudes of vibration.

B) Computer Analysis of the Data: - The plots of porosities versus amplitude of vibrations show wide scatter. In view of the limited number of observations and very





small range of amplitudes studied, it was decided to force fit a straight line through the data by means of a computer.

The relationship was supposed to be of the nature,

$$C = \phi + B Z a$$

where B and C are constants. For n observations, the summation is

$$nC = \Sigma \phi + B \Sigma Z a$$

$$\therefore C = \frac{\Sigma \phi + B \Sigma Z a}{n} \quad (1)$$

Multiplying throughout by Za, we get

$$Z a \cdot C = \phi Z a + B Z a^2$$

$$\text{and } C \Sigma Z a = \Sigma \phi Z a + B \Sigma Z a^2$$

From these we have,

$$B = \frac{\Sigma \phi Z a - \frac{\Sigma \phi \cdot \Sigma Z a}{n}}{\frac{(\Sigma Z a)^2}{n} - \Sigma Z a^2}$$

The results and the standard deviation of the data are shown in Table 3 of the Chapter "Results".

C) Calculation of Permeability: - The measured quantities were time for 250 c.c. in minutes, the height of the pack observed, and the pressure differential noted in the  $\text{CCl}_4\text{-H}_2\text{O}$  differential manometer. The method of computation of permeability was simplified by modifying the relationship 14a. The density of



$\text{CCl}_4$  was 1.587 gms/c.c. The manometer read in inches. For vertical flow, the total pressure differential across the core was

$$\begin{aligned}\Delta P_w &= (1.587 - 1) 2.54 \Delta P_{\text{obs}} \\ &= 1.482 \Delta P_{\text{obs}}\end{aligned}$$

From the time of 250 c.c.'s of flow, we obtain flow rate in c.c./min. by the relationship,  $q = 250/60t$ . The area of cross section of cell was 20.1488 sq.cm. and the viscosity of water was 1 c.p. Applying all these in relationship 14a, we get

$$\begin{aligned}K &= \frac{q \mu L \times 1033.6}{A \Delta P_w} \\ &= 250/60t \times 1/20.1488 \times L/(1.482 \Delta P_{\text{obs}}) \\ &= 213.9 L/t(1.482 \Delta P_{\text{obs}}) \\ &\approx 144 \frac{L}{t \Delta P_{\text{obs}}}\end{aligned}$$

The values thus calculated were reported up to 2 significant figures in Tables 6 and 7 for Big beads and Ottawa sand.



TABLE 1

Determination of Porosity of Packs ofBig Beads

Amp Set	Wt. gms	ht. cm	Bulk Vol. c.c.	Wt. of Bulk gm	$\rho_a$ gm/cc	$\phi$ %
3	3830.8	0.656	274.47	536.40	1.954	33.75
5	3830.2	0.520	271.76	536.20	1.973	32.45
7	3824.4	0.470	270.75	530.4	1.959	33.43
10	3832.2	0.640	274.37	538.2	1.962	33.25
8	3845.7	0.975	280.90	551.7	1.964	33.08
15	3823.2	0.480	270.95	529.2	1.953	33.84
12	3838.2	0.765	276.68	544.2	1.967	32.88
5	3834.2	0.700	275.36	540.2	1.962	33.23
7	3832.4	0.745	276.28	538.4	1.949	34.14
3	3832.0	0.680	274.97	538.0	1.957	33.59
5	3832.0	0.670	274.77	538.0	1.958	33.49
10	3842.8	0.890	279.19	548.8	1.966	32.96
1	3824.0	0.500	271.36	530.0	1.953	33.84
0	3811.6	0.175	264.83	517.6	1.955	33.74
10	3799.5	2.135	254.88	497.56	1.9521	33.90
20	3777.8	0.835	228.76	449.74	1.966	32.94
Om	3744.10	1.375	197.02	384.295	1.9533	33.84
20	3780.9	0.860	229.26	543.34	1.977	32.15
10	3769.5	0.570	223.43	436.11	1.952	33.92
22	3776.62	0.665	225.35	445.15	1.975	32.29
15	3774.03	0.790	227.86	445.07	1.9599	33.37
0	3913.83	0.82	229.09	450.80	1.068	32.82
25	3913.75	0.67	226.07	447.695	1.9803	31.94
10	3919.70	1.81	227.81	445.38	1.955	33.70
15	3921.545	1.035	233.42	462.66	1.982	31.82
25	3925.9	1.025	233.22	467.00	1.9881	31.41





TABLE 2

Determination of Porosity of Packs of  
Ottawa Sand

$$\rho = 2.6513 \text{ gms/cc.}$$

$$\text{dia} = .0825 \text{ cm}$$

Amp Set	Wt. gms	ht. cm	Bulk Vol c.c.	Wt. of Pack (gm)	$\rho_a$ gm/cc	$\phi$ $Z$
Omax	3850.2	0.205	265.43	556.2	2.096	33.66
15	3815.6	1.095	233.99	492.79	2.106	33.02
17	3795.73	0.130	214.60	453.50	2.113	32.58
12	3801.82	0.480	221.63	466.63	2.1054	33.06
20	3808.65	0.650	225.04	476.88	2.119	32.23
10	3789.40	1.785 cm both	205.25	434.32	2.116	32.41
25	3931.92	2.095 both	212.07	451.90	2.131	31.51
20	3951.72	0.88	230.30	489.90	2.127	31.74
25	3943.25	0.44	221.44	472.56	2.134	31.32
17	3950.42	0.865	230.00	488.29	2.123	31.99
15	3958.32	1.310	238.97	505.16	2.114	32.54
12	3942.03	0.995	232.62	481.62	2.1134	32.57
0	3920.0	1.96*	209.35	436.32	2.0842	34.34
3	3941.62	0.845	229.60	478.19	2.0827	34.43
5	3939.25	0.575	224.16	470.38	2.0984	33.48
0	3942.25	0.77	228.08	477.30	2.027	34.83
15	3947.54	0.81	228.89	483.30	2.1119	32.67
22	3942.25	0.81	228.89	488.11	2.1325	31.42
10	3949.65	0.895	230.60	487.22	2.1128	32.61
10	3944.67	0.735	227.38	478.42	2.1041	33.14
1	3922.350	-0.05	211.56	440.88	2.0839	34.36
7	3927.855	0.08	214.18	449.005	2.0964	33.60



TABLE 3

Determination of Porosity of Packs ofMedium Beads

dia = 0.05183 cm

 $\rho = 2.590 \text{ gm/cc}$ 

Amp Set	Wt. gm	ht. of ex- tension project- ing out cm.	Bulk Vol. c.c.	Wt.of Pack gms	$\rho_a$ gm/cc	$\Phi$ (%)
3	3855.50	0.78	276.98	561.5	2.027	35.40
5	3851.50	0.67	274.77	557.5	2.029	35.29
20	3856.80	0.685	275.07	562.8	2.046	34.21
12	3839.80	0.405	269.45	545.8	2.026	35.50
5	3832.00	0.265	266.63	538.0	2.018	35.86
17	3859.20	0.790	277.18	565.2	2.039	34.65
25	3864.10	0.855	278.49	570.1	2.047	34.14
8	3840.20	0.390	269.15	546.2	2.029	35.25
22	3864.00	0.915	279.70	570.0	2.038	34.72
Omax	3840.70	0.430	269.95	546.7	2.025	35.55
3	3829.60	0.250	266.33	535.6	2.011	36.42
7	3848.20	0.580	272.96	554.2	2.030	35.20
5	3842.80	0.506	272.38	548.8	2.015	36.18
Omax	3800.10	1.385	239.8	483.1	2.015	36.19
20	3805.22	1.430	240.71	489.81	2.035	24.91
15	3805.40	1.290	237.90	486.98	2.047	34.15
1	3801.91	1.530	242.72	488.31	2.012	36.36
10	3787.90	0.700	226.04	457.12	2.022	35.70
1	3991.69	0.780	276.98	561.500	2.027	35.40
10	3995.39	9.790	277.18	565.20	2.039	346.65
15	3984.39	0.580	272.96	554.20	2.030	35.20
12	4000.31	0.855	278.49	570.12	2.047	34.14



TABLE 4

Determination of Porosity of Packs ofSmall Beads

$$\text{dia} = 171.4 \mu$$

$$\rho = 2.4404 \text{ gms/cc.}$$

Amp Set	Wt. gms	Ht. cm	Bulk Vol. c.c.	Wt. of Pack gms	$\rho_a$ gms/cc.	$\phi$ %
Omax	3805.6	0.19	266.3	511.6	1.9209	36.05
15	3808.0	0.205	265.43	514.00	1.9365	34.99
12	3823.8	0.639	274.1	529.8	1.9331	35.20
5	3814.2	0.420	269.8	520.2	1.9285	35.52
7	3809.6	0.345	268.3	515.6	1.9222	35.96
10	3826.2	0.640	274.2	532.2	1.9411	34.65
8	3814.0	0.430	269.95	520.0	1.9262	35.68
Omax	3822.2	0.585	273.1	528.2	1.9344	35.11
10	3822.2	0.610	273.6	528.2	1.9308	35.36
3	3834.0	0.945	280.30	540.0	1.9240	35.82
17	3837.3	0.880	279.0	543.3	1.9474	34.21
5	3812.0	0.365	268.65	518.0	1.9282	35.54
25	3919.70	1.81	227.81	445.38	1.955	33.70
20	3962.40	0.640	274.20	532.21	1.9411	34.65
1	3964.61	0.745	276.28	534.42	1.9295	35.40
7	3944.50	0.205	265.43	514.31	1.9370	34.94
15	3965.37	0.680	274.97	535.18	1.9441	34.45
25	3973.52	0.880	279.00	543.33	1.9476	34.23



TABLE 5

Determination of Porosity of Pack ofBROWN BEADS

$$\rho = 2.562 \text{ gm/cc.}$$

$$\text{dia} = .01418 \text{ cm}$$

Amp Set	Wt. gm	Ht. cm	Bulk Vol. c.c.	Wt. of Pack gm	$\rho_a$ gm/cc.	$\phi$ %
12	3853.7	0.83	276.99	559.7	2.001	35.65
5	3838.3	0.535	272.06	544.3	2.001	35.93
7	3837.2	0.650	274.37	543.2	1.980	37.27
3	3825.8	0.320	267.71	531.8	1.987	36.84
10	3840.2	0.610	273.57	546.2	1.997	36.20
1	3849.8	0.840	278.19	555.8	1.998	36.11
Omax	3831.8	0.465	270.65	537.8	1.987	36.81
7	3832.0	0.400	269.35	538.0	1.997	36.15
10	3850.2	0.810	277.59	556.2	2.004	35.74
1	3844.2	0.705	275.48	550.2	1.997	36.16
5.0	3825.8	0.320	267.71	531.8	1.9865	36.84
15	3930.0	1.22	237.15	474.12	1.9992	36.03
30	3933.20	1.38	240.38	480.55	1.9991	36.04
20	3919.8	0.64	225.47	452.24	2.0058	35.61
17	3918.3	0.60	224.66	449.93	2.0027	35.81
12	3954.45	0.24	263.35	524.26	1.9907	36.57
18	3940.1	1.60	244.81	491.88	2.0092	35.39
13	3947.17	1.82	249.24	503.38	2.0197	34.72
22	3926.88	0.89	230.50	464.35	2.0145	35.05
25	3947.8	1.885	250.55	505.32	2.0168	34.90





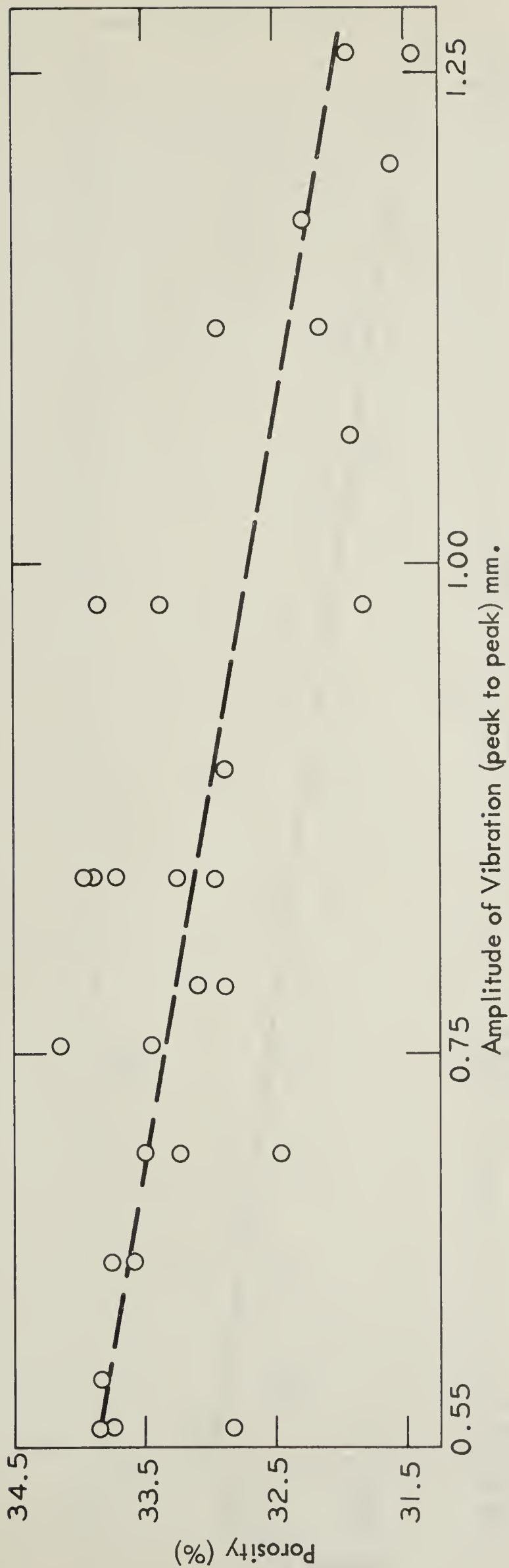


FIG. 4. EFFECT OF AMPLITUDE OF VIBRATION ON POROSITY OF BIG BEAD PACKS

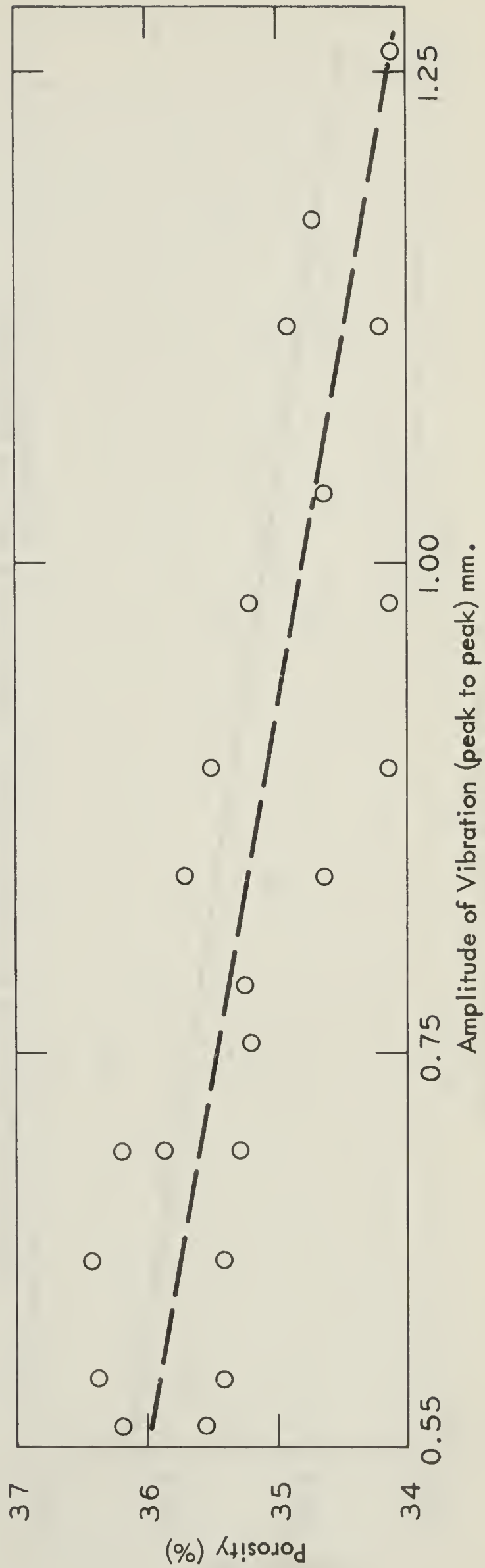


FIG. 5. EFFECT OF AMPLITUDE OF VIBRATION ON POROSITY OF MEDIUM BEAD PACKS



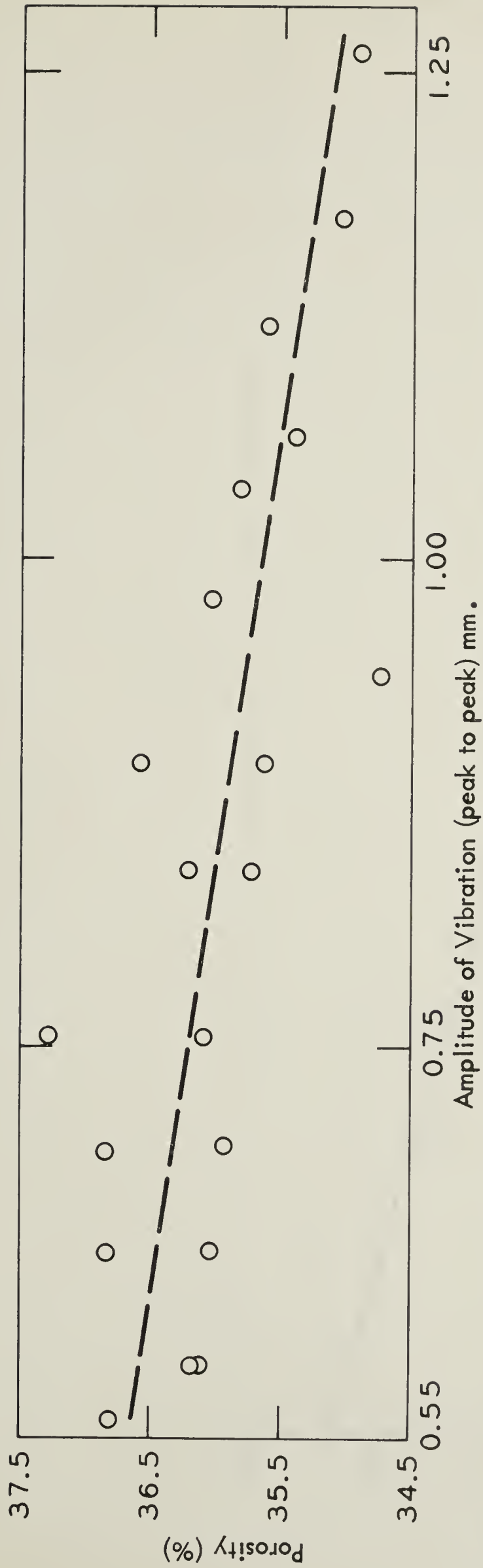


FIG. 6. EFFECT OF AMPLITUDE OF VIBRATION ON POROSITY OF BROWN BEAD PACKS

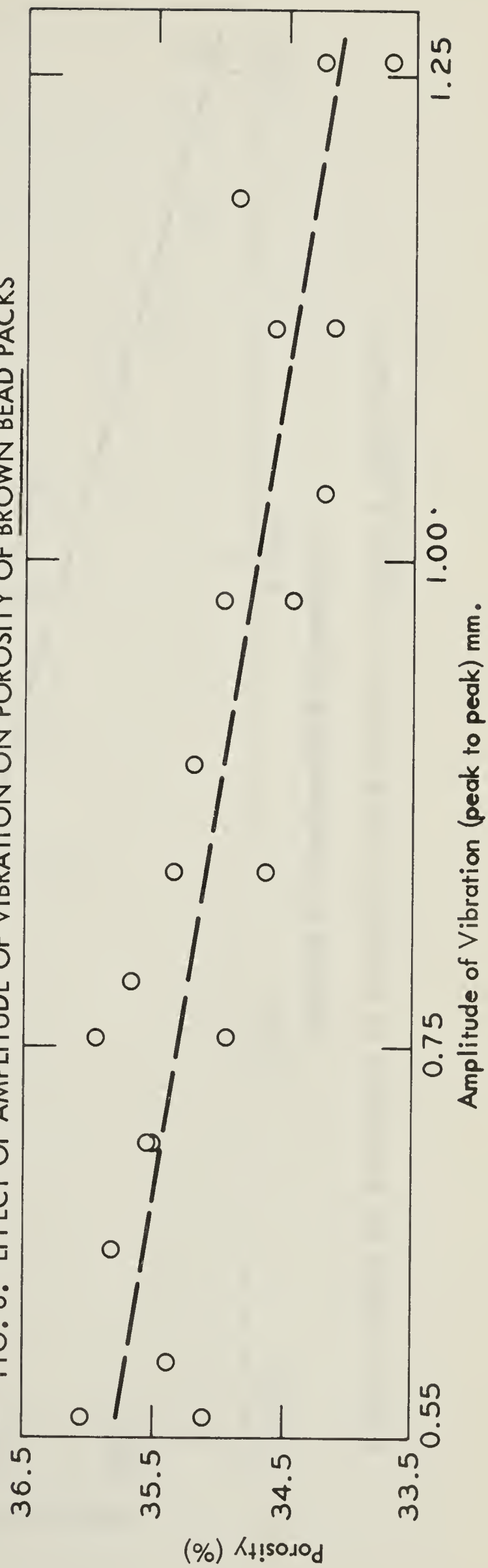


FIG. 7. EFFECT OF AMPLITUDE OF VIBRATION ON SMALL BEAD PACKS



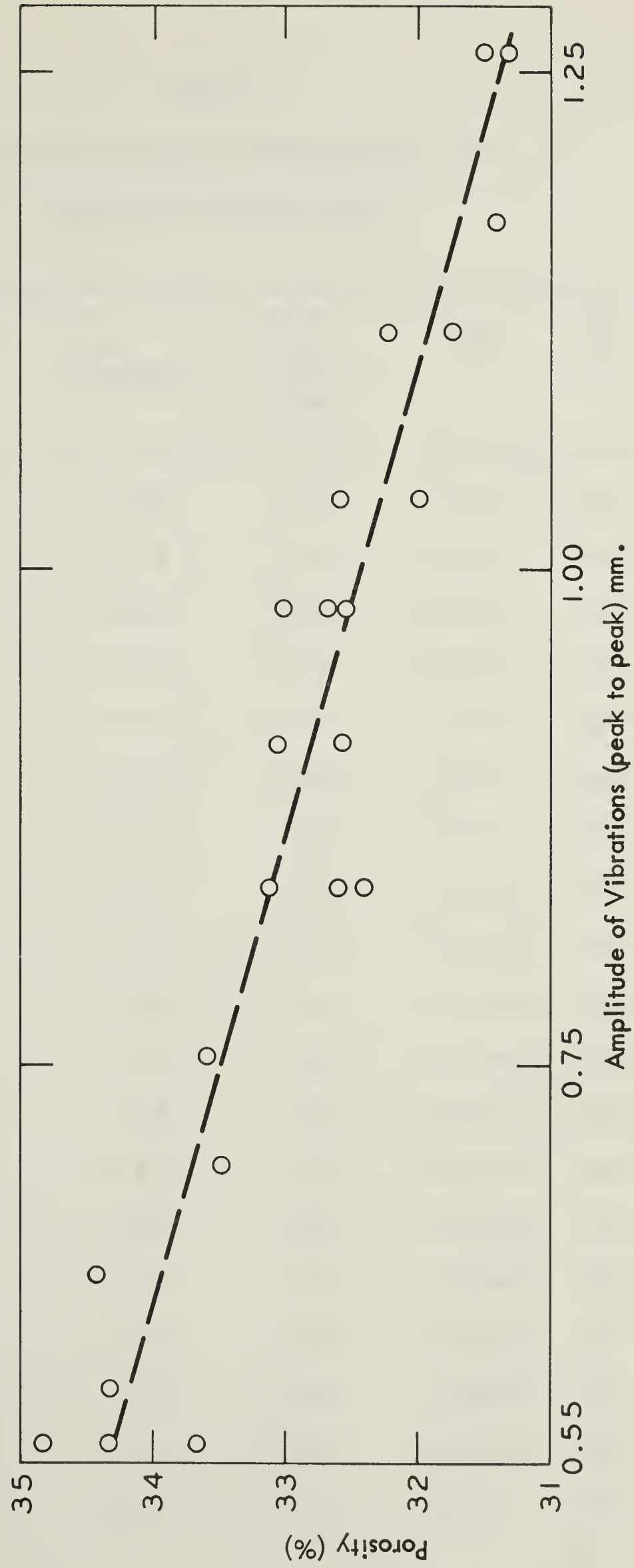


FIG. 8. EFFECT OF AMPLITUDE OF VIBRATION ON POROSITY OF OTTAWA SAND PACKS





TABLE 6

Determination of Permeability of  
Packs of Ottawa Sand

Amp Set	ht <sub>obs.</sub> (cm)	P <sub>obs</sub> (inches)	time for 250cc Flow (Min)	L (cm)	K (d)	$\phi$ %
12	0.480	3.20	3.84	11.03	131	33.06
20	0.650	3.18	2.32	11.20	218	32.23
10	1.785	4.01	2.30	10.205	160	32.41
25	2.095	5.07	2.53	10.525	120	31.51
20	0.88	6.26	2.05	11.430	128	31.74
25	0.44	4.62	2.08	10.99	165	31.32
7	0.08	5.21	2.18	10.63	136	33.60
17	0.865	2.43	4.95	11.415	137	31.99
15	1.310	6.75	1.79	11.860	141	32.54
12	0.995	2.20	2.62	11.545	288	32.57
0	1.96	3.75	1.80	10.390	221	34.34
3	0.845	3.12	1.82	11.395	278	34.43
5	0.575	2.60	2.48	11.125	249	33.48
0	0.77	2.20	1.90	11.320	390	34.83
15	0.81	2.50	2.32	11.360	282	32.67
22	0.81	2.50	2.41	11.360	272	31.42
10	0.895	3.56	1.83	11.445	252	33.62
10	0.735	2.35	2.54	11.285	272	33.14
1	-0.050	2.00	2.20	10.50	344	34.36



TABLE 7  
Determination of Permeability of  
Packs of Big Beads

Amp Set	ht. obs (cm)	$\Delta P$ obs (inches)	Time for 250cc. Flow (Min)	L (cm)	$\Delta P_w$ (cm)	K (d)	$\phi$ %
10	2.135	1.32	2.81	12.685	491		33.90
20	0.835	1.07	2.53	11.385	605		32.94
0	1.375	1.05	2.38	11.925	688		33.84
20	0.860	1.2.	2.58	11.41	532		32.15
10	0.570	1.11	2.47	11.12	585		33.92
22	0.665	1.16	2.14	11.215	653		32.29
15	0.790	1.02	2.36	11.34	680		33.37
0	0.82	1.05	1.93	11.370	808		32.82
25	0.67	1.43	2.54	11.220	445		31.94
10	1.8.	0.87	4.37	12.360	468		30.70
15	1.035	1.15	2.94	11.585	493		31.82
25	1.025	1.11	2.86	11.575	525		31.41
8	0.445	1.20	2.03	10.995	650		32.88
18	0.280	1.40	2.15	10.830	519		31.93
23	0.620	1.07	2.57	11.17	585		31.58



## PART II

### SIMULATION OF WETTABILITY CONDITIONS



## THEORY AND LITERATURE REVIEW

### A. Wettability and Surface Forces

Wettability, qualitatively speaking, denotes the ease with which a fluid can displace other fluids, or spread over a solid surface in the presence of other fluids.

The cohesion between the molecules of a liquid must surpass their tendency to separate under the influence of thermal motion. This net attraction between neighbouring atoms is fulfilled most completely in the interior of the phase while those molecules at the surface are attracted less completely than they would have been in the bulk. Consequently the latter has greater energy. At equilibrium, the free energy of the surface, which is the maximum energy available for performing work, tends to assume the minimum possible value. If there are two or more phases in contact, the free energy at any interface will reach a minimum value, provided, that in so doing, it does not tend to raise other energy values within the system. At equilibrium conditions the interfaces and the free surfaces are thus under stress.

Consider a solid surface  $S$  (figure 1) with fluid  $A$  spreading over it, in the presence of fluid  $B$ . An areal element of the  $S/B$  interface is replaced by an equal area of the  $S/A$  interface and is generally also accompanied





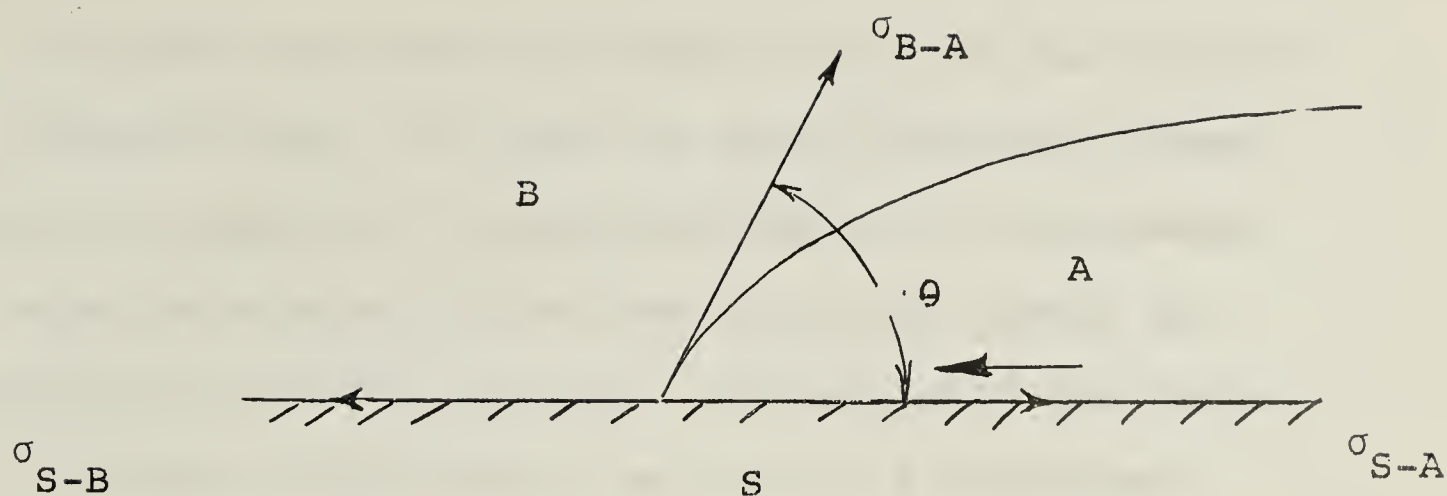


Fig. 1

by an extension of the A/B interface. These conditions may change progressively as the wetting proceeds. Each interface has its own specific surface energy content. Wetting with an accompanying change in the areal extent of each interface, results in a net change in the total surface energy. The magnitude of this change in net energy determines the rate at which the wetting would proceed. The net energy change is equivalent to the work of adhesion, i.e. the work involved in the substitution of an S/A interface by an equal S/B interface.

In wettability analysis, the force rather than energy concept is used for the sake of simplicity. The forces are assigned values numerically equal to characteristic (specific) interfacial energy values and are dealt with as vectors.

Since the natural tendency of two liquids in contact is to decrease the interface, any increase in



interface can only be accomplished with the expenditure of work. The work in ergs (dynes/cm) necessary to generate a square centimeter of interfacial area is referred to as free interface energy per square centimeter of area. Consequently the force in dynes acting along 1 cm length of interface is referred to as interfacial tension. The interfacial tension acts on the interface. In the above case where fluid A is spreading in the presence of B, the system is in a state of equilibrium and the force balance is given by

$$\sigma_{S-B} = \sigma_{S-A} + \sigma_{B-A} \cos \theta \quad (1)$$

where

$$\sigma = \text{Interfacial tension}$$

$$\theta = \text{Contact angle between the solid and the interface, as measured through the wetting phase B.}$$

[S, B and A as suffixes denote solid and fluid B and A respectively].

Adhesion tension  $A_T$  is the difference in the interfacial tension between the solid and the two liquid phases and is given by

$$A_T = \sigma_{S-B} - \sigma_{S-A} = \sigma_{B-A} \cos \theta_{A-B} \quad (2)$$

A positive adhesion tension indicates that the solid surface is preferentially wetted by the incumbent phase.





From the above relationship, it follows that for the adhesion tension to be positive,  $\cos \theta$  must be positive i.e.  $\theta$  should be less than  $90^\circ$  (as measured through the incumbent phase).

Since the free energy of a system always tends to a minimum, surfaces have a tendency to adsorb different molecules which may partly or wholly balance the unsatisfied forces. Polar impurities and many vapours adsorb on surfaces, forming films, which might have condensed from the vapour phase or migrated from liquid drops over the surface. The adsorbed components decrease the adhesion tension at the surface and are generally referred to as contaminants.

Wenzel (1) has shown that the measured value of  $\theta$  is influenced by roughness of the solid surface. Due to roughness of many kinds, the actual surface area of a rough solid surface is much larger than the apparent plane area of the surface. If the actual surface area is  $x$  times the apparent plane area, the measured contact angle  $\bar{\theta}$  is given by

$$\cos \bar{\theta} = x \cos \theta \quad (3)$$

where  $\theta$  is the true contact angle.

It may be noted that  $\bar{\theta} > \theta$  for  $\theta < 90^\circ$  and  $\bar{\theta} < \theta$  for  $\theta > 90^\circ$ .

Cassie and Baxter (2) point out a similar effect





in the case of roughness caused by the occurrence of pores in a system.

If the order of displacement of fluid be changed, it is observed that the contact angles measured through a particular phase in the two cases are different. The effect is known as hysteresis and many possible explanations have been offered.

Adam (3) lists a few of them. If the surface is covered by some contaminant films and one of the two phases preferentially adsorbs them, the contact angles in the two cases are likely to be different. Likewise, the formation of multimolecular clusters by the receding liquid on the solid surface would lead to the hysteresis of contact angles. Surface roughness permits the droplets of the receding phase to occupy states, where the surface energy has a subsidiary minima different from the absolute minimum, and this would lead to a different value of adhesion tensions in the two cases.

It is very obvious that adhesion tension is a specific property, depending upon the phases involved, contamination and surface histories.

It is necessary, therefore, that while quantitatively reporting wettability the three phases involved and the direction of movement (displacement) of fluids be specified.



No specific quantitative scale for reporting wettability is available as yet; however the values of adhesion tension ( $A_T$ ),  $\cos \theta$ , or the contact angle ( $\theta$ ) are generally used as indices of wettability. Sometimes, "Wettability Number" or "Wettability Index" (W) which is a ratio of the measured adhesion tension to some standard value of adhesion tension is also used for that purpose.



## B. NATURE OF GLASS SURFACES

The surface properties of glass depend upon its structure, bulk composition and surface history. Fresh glass surfaces exhibit attractive forces due to unbalanced ions on their surfaces. The surfaces of freshly blown glasses stick, when they are brought together. Clean glass surfaces have been long known to be hydrophylic; the contact angles for water-air system being reported as  $0^\circ$  (4).

Some substances combine chemically with glass surfaces so that forces arise from electrovalent or covalent bonds. The high adhesion of metal oxide coatings to glass can be explained by the tendency of the glass to continue its network structure with the atoms in metal oxides. Organic molecules, having unsaturated groups or polar radicals, tend to orient themselves in such a way that these groups or radicals point toward the glass surfaces. This phenomenon results in glass surfaces satisfying all or some of the unsaturated bonds and changing their wettability. Contaminated glass surfaces can be cleaned to restore their original wetting conditions. One such cleaning method, suggested by Polak and Wendler (5) involves thorough washing with an organic solvent, followed by immersing the glass bodies in hot chromic acid for 18 hours. The acid traces may be removed by rinsing with





distilled water and any volatile impurities still sticking to the surfaces may be removed by exposing the surfaces to a glow discharge lamp for half an hour.

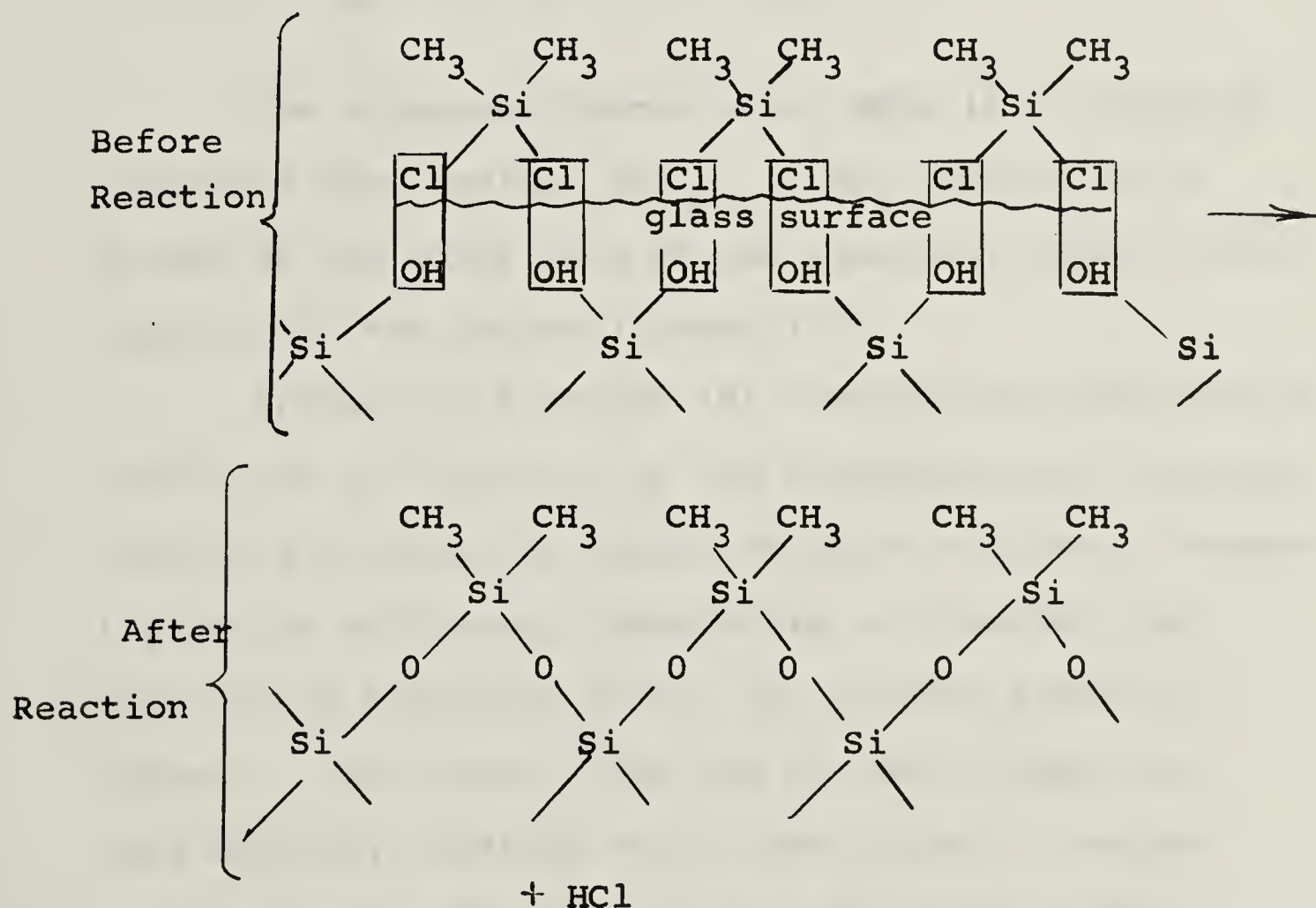
Chemisorbed silicones on the surface can best be removed by heating the glass surface to some temperature near its annealing point.

The contact of water vapours with the glass surface forms some type of silica gel containing negatively charged siloxyl group ( $\text{SiOOH}^-$ ) having one free bond to be further satisfied by other substances coming in contact with it. Oxygen molecules coming in contact with such a surface get themselves adsorbed over it, forming a film. The reaction of a polar compound containing organic as well as inorganic radicals with the surface film may modify the surface in such a way that inorganic radicals will be attracted toward it, with organic radicals propping outwards. This phenomenon produces hydrophobicity of the glass surface. If the polar group happens to contain silicon, the bond is likely to be irreversible; and the film mechanically strong and heat resistant. Silicones are one group of such compounds. They are polymers or monomers of molecules containing alternate silicon and oxygen atoms, the silicon atoms having some organic groups such as methyl or phenyl radicals attached to them. Substitution of some of these organic groups or oxygen





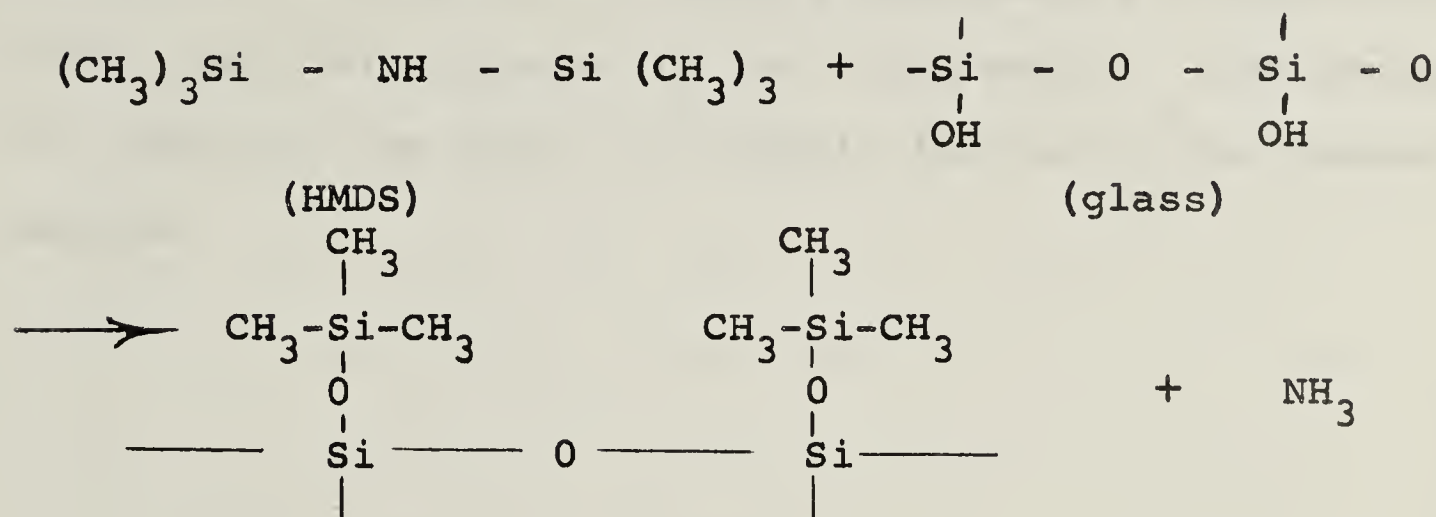
atoms by alkoxyl, hydroxyl groups, or atoms of Hydrogen or chlorine make such fluids chemically more active, and the fluids are termed organo-functional silicones. Dow-Corning fluids used in the work belong to this group. They react with the adsorbed water on the glass surface of  $\text{OH}^-$  groups, facilitating silicon atoms to link with the glass structure. The reaction may be represented as:



The new surface has water repellent  $\text{CH}_3$  (or other organic) groups outermost. The bond can be destroyed only by destructive methods such as treatment with hydrofluoric acid or heating the glass to annealing temperatures. (6)



The other compound used in this study was Hexamethyl disilazane (HMDS) which reacts with glass surfaces in the same way as silicones -



The bidentate character of HMDS is no drawback since the free radical  $(\text{CH}_3)_3\text{Si NH}_2$  appears to be formed in the first step of the reaction, which itself reacts with the hydroxyl group (7).

Spitze and Richards (8) studied the influence of the conditions of treatment on the hydrophobicity obtained. According to them, the nature of glass surfaces, concentration of silicones, temperature of treatment and duration of treatment affect the contact angles obtained. They report that due to their higher surface activity, glasses with higher alkali content would allow the fluids to orient themselves more quickly and attach themselves more strongly, producing relatively higher contact angles. Higher concentration of silicones would provide a coverage of the surface many molecules thick. At higher temperatures, the silicones



would disintegrate and leave the surfaces rougher due to the deposition of silica. The contact angles of treated surfaces through the water phase increase as the temperature of treatment is increased; but at a temperature of approximately  $500^{\circ}\text{C}$  the disintegration of the fluid begins. The prolongation of reaction time helps in slightly increasing the contact angles.







### C. MEASUREMENT OF WETTABILITY

Contact angle is one of the most widely used indices of wettability. Contact angles can be directly measured on flat surfaces or computed from dimensions of a drop; however, in the case of a porous medium, the direct measurement is impractical, if not impossible. Two very sophisticated methods have been proposed in recent years, for the determination of the wettability of porous media. One is a Dye Adsorption method proposed by Holbrook (9) and the other is a Nuclear Magnetic Relaxation method, proposed by Brown and Fatt (10). Both are based on the assumption that due to adsorption of polar compounds, some part of the total area is completely oil wet, while the other part is completely water wet and the ratio of the two areas are manifested by different contact angles. The methods have not gained wide-spread acceptance because of the uncertainty about the validity of the assumptions.

Bobek, Mattax and Denekas (11) propose a dynamic method for the semi-quantitative determination of wettability. They propose that the spontaneous imbibition of the wetting phase by a porous medium is closer to the actual case of flow and is greatly influenced by wettability conditions. The method provides only qualitative information, since no method



is available for determining values of adhesion tension or contact angles from the measurements taken during these tests.

Visual examination of a porous medium containing two fluids in the void spaces indicates that the interface between the fluids is slightly curved. This curvature is guided by the size (crosssectional area) and shape of void spaces at different points, and by the properties of the two fluids present. The curvature is a consequence of different pressures on the two sides of the interface. At zero pressure differential, the interface will show zero curvature i.e. the interface will be flat (12). This suggests an analogy between porous media and capillary rise in a tube of small bore and hence the pressure differential is called capillary pressure. From the magnitude of capillary pressure, the adhesion tension and hence the contact angles can be computed for the rise of fluid in a circular capillary tube, in the following way. The upward acting force, at a capillary column, due to adhesion tension will be  $2\pi r.A_T$ , where  $r$  is the radius of the capillary; whereas the downward acting force due to gravity will be  $\pi r^2 h \Delta \rho g$  where  $h$  is the capillary rise in the tube,  $\Delta \rho$  is the difference in densities of the two phases and  $g$  is acceleration due to gravity. The product  $h \Delta \rho g$



is the capillary pressure  $P_c$  and hence we have, at equilibrium,

$$\begin{aligned} 2\pi r A_T &= \pi r^2 P_c \\ A_T &= \frac{P_c \cdot r}{2} \end{aligned} \quad (4a)$$

From equation 2,  $A_T = \sigma_{AB} \cos \theta$

$$\cos \theta = \frac{P_c \cdot r}{2\sigma_{AB}} \quad (4b)$$

$$\text{or } \theta = \cos^{-1} \frac{P_c \cdot r}{2\sigma_{AB}} \quad (4c)$$

Plateau (13) has shown that in the case where uniform spheres constitute the porous medium, the mean capillary radius  $r$  for the pore spaces can be computed from  $r_1$  and  $r_2$  (figure 2) by the relation:

$$\frac{1}{r} = \frac{1}{r_1} + \frac{1}{r_2} \quad (5)$$

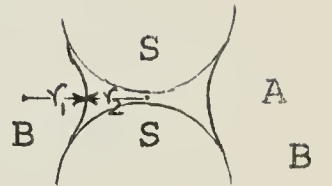


Fig 2.

It is not feasible to measure the values of  $r_1$  and  $r_2$  and hence attempts have been made to compute the value of  $r$  from other properties.

Assuming no dead end pores; pores distributed at random and reasonably uniform in size; porosity not very high and diffusion and surface effects absent; Carman (14) derived a relationship between average pore radius, diameter of sphere and the porosity  $\Phi$  [based on hydraulic diameter concept] which is;





$$r = \frac{\phi d}{3(1-\phi)} \quad (5a)$$

Since no factors to account for geometrical configuration appear in this relationship, it appears that the relationship is rather an oversimplification; besides, it is very much open to meniscus errors.

Leverett (15) reports yet another relationship for determining the mean pore radius, based upon Darcy's and Poiseuille's law, which seems to be more widely accepted. The porous medium is simulated by a bundle of circular, straight and identical capillary tubes, which in bulk would have the same porosity ( $\phi$ ) and permeability ( $K$ ), as the porous medium. This model yields the following relationship for values of mean pore radius:

$$r = 2.815 \times 10^{-4} \sqrt{\frac{k}{\phi}} \quad (6)$$

Perhaps this relationship is also an oversimplification, but it takes into account the geometrical complications. It is possible that the exact relationship between mean pore radius, porosity and permeability may be similar in nature as is the above relationship. It is also possible that during the process of reverse transformation of capillary tube analogy to an actual porous medium, the numerical constant in the above relationship may be modified as a result of geometrical complications.





Based upon the above concept of analogies between porous media and capillary tubes, Bartell and Osterhof (16) proposed a method for the determination of capillary pressure. They packed granules into a cell and the minimum pressure at which a fluid entered the porous medium was designated the threshold pressure i.e. the pressure required to overcome capillary resistance. The values of contact angles were computed from the relationship 4 c. Slobod and Blum (17) improved the experimental technique and tried to eliminate the mean pore radius by introducing wettability number W" and "Apparent Contact Angle" which may be determined from the relationship

$$W = \left[ \cos \theta_{o-w} \right]_{\text{apparent}} = \frac{\cos \theta_{o-w}}{\cos \theta_{a-o}} = \frac{\sigma_{a-o}^p C_{o-w}}{\sigma_{o-w}^p C_{a-o}} \quad (7)$$

[suffixes a, o and w represent air, oil and water]

It is apparent that both air-oil displacement and oil-water displacement must take place on the same porous medium for the above relationship to be valid. Since the reproduction of geometry of a porous medium is highly unlikely with the available packing techniques, the above method is not free from geometric errors.

Faris and Whalen (18) while discussing the above



paper note that since the capillary pressure measured as above takes into account only the largest capillaries at the face of the fluid entrance, they are far from being average values for the entire porous medium. The assumption of mean capillary radius severely limits the extension of capillary pressure values to smaller capillaries.

The relationship obtained for static conditions may not be applicable for dynamic (flow) conditions. Adam (19) has shown that the geometry of the capillaries greatly influences the nature of interface advance and attendant displacement (capillary) pressures. Calhoun (20) argues that the test is not a positive test as the lack of imbibition does not indicate non-wetting by the displacing phase, while the reverse is true. In addition a positive pressure differential is more apt to be required, even in the case where the medium contains none of the wetting phases at the beginning of the test. The technique used in the present investigation was a modification of the above displacement measuring technique.





## EXPERIMENTAL STUDIES

### 1. WETTABILITY DETERMINATION

#### A) Design of Experiments:

From the considerations of the preceding chapter, it was decided that the wettability studies be based upon measurement of displacement pressure. The mean pore radii, as they might be varying in different tests, were to be accounted for, from the data of porosity and permeability. From the considerations of uncertainty about constant of proportionality in equation 5, (between mean pore radius  $r$  and  $\sqrt{\frac{K}{\phi}}$ ), it was decided that the concept of wettability number  $W$  incorporating ratios of radii be used. From equation 5, the ratio of radii would be the same as that of corresponding ( $\sqrt{\frac{K}{\phi}}$ ). Therefore, it was decided that a pack of the cleanest possible beads be used as a reference. The glass beads were cleaned, by the method suggested by Pohlack and Wendler(21) with slight modifications. The procedure of cleaning is described elsewhere in this chapter.

It is believed that the resulting contact angle through water on a glass surface thus cleaned, may not be very different from zero. In view of the uncertainty of the above factor, an apparent contact angle concept was used, based upon the assumption that the cleanest possible surface had  $0^\circ$  contact angle. The





relationship used was

$$w' = \cos \theta = \frac{P_{c_o}}{P_{c_r}} \cdot \frac{\sigma_{o-w_r}}{\sigma_{o-w_o}} \cdot \sqrt{\frac{K_o \phi_r}{K_r \phi_o}}$$

Here  $w'$  = modified wettability number (8)

$\theta$  = Apparent contact angle.

Suffixes o and r refer to properties of sample under observation and the reference sample (cleanest possible).

Although the procedure still retains many of the drawbacks mentioned earlier, it was expected that it should be able to furnish, to a satisfactory degree, the information required about the wettability of the surfaces of glass beads, treated with different amounts of silicone fluid and HMDS.

The variables required to be measured were (according to equation 8), capillary pressures, interfacial tensions, permeabilities and porosities of packs of glass beads. The determination of porosity and permeability, in turn required information regarding temperature, viscosity, flow rate, volume, weight and length of the pack and specific gravity of glass beads during different tests. Due to considerations of simplicity, it was decided that the experiments be conducted at atmospheric pressure and since the effect of changes in temperature on the values of contact angles is very slight (less than 1/3 of a degree per degree Fahrenheit change of temperature), no temperature control-



ling devices were used.

### B) Apparatus.

A ruska rate constant proportioning pump was used along with a flow reduction assembly, which isolated injection fluid from mercury. The pressure across the cell was measured using a differential pressure transducer [Statham - model PM80TC]. The pressure transducer converted pressures into voltage signals, which were recorded continuously by a voltage recording device. For the earlier few studies a Honeywell viscicorder Recorder [model 906-C] was used and later, for better magnification of voltage signals, a Beckman R.S. Dynograph was used. The transducer was excited by a D.C. current supplied by a Kepco SC18-1 rectifier - transformer type of power system. A vacuum pump was attached to the unit to evacuate the system before the entry of fluids. Figure 3 shows the experimental set-up. The flow reduction unit consisted of two stainless steel cylinders with a common plunger, having different diameters on two sides, moving in them. All the connections were made with autoclave (1/8") tubing in order to avoid corrosion by the brine solution. The test cell was made of glass and all accessories were made of high grade Lucite and Teflon, in order to avoid any contamination - corrosion problems. The cell was 3.65 cm dia x 12.25 cm long. The brine reservoir



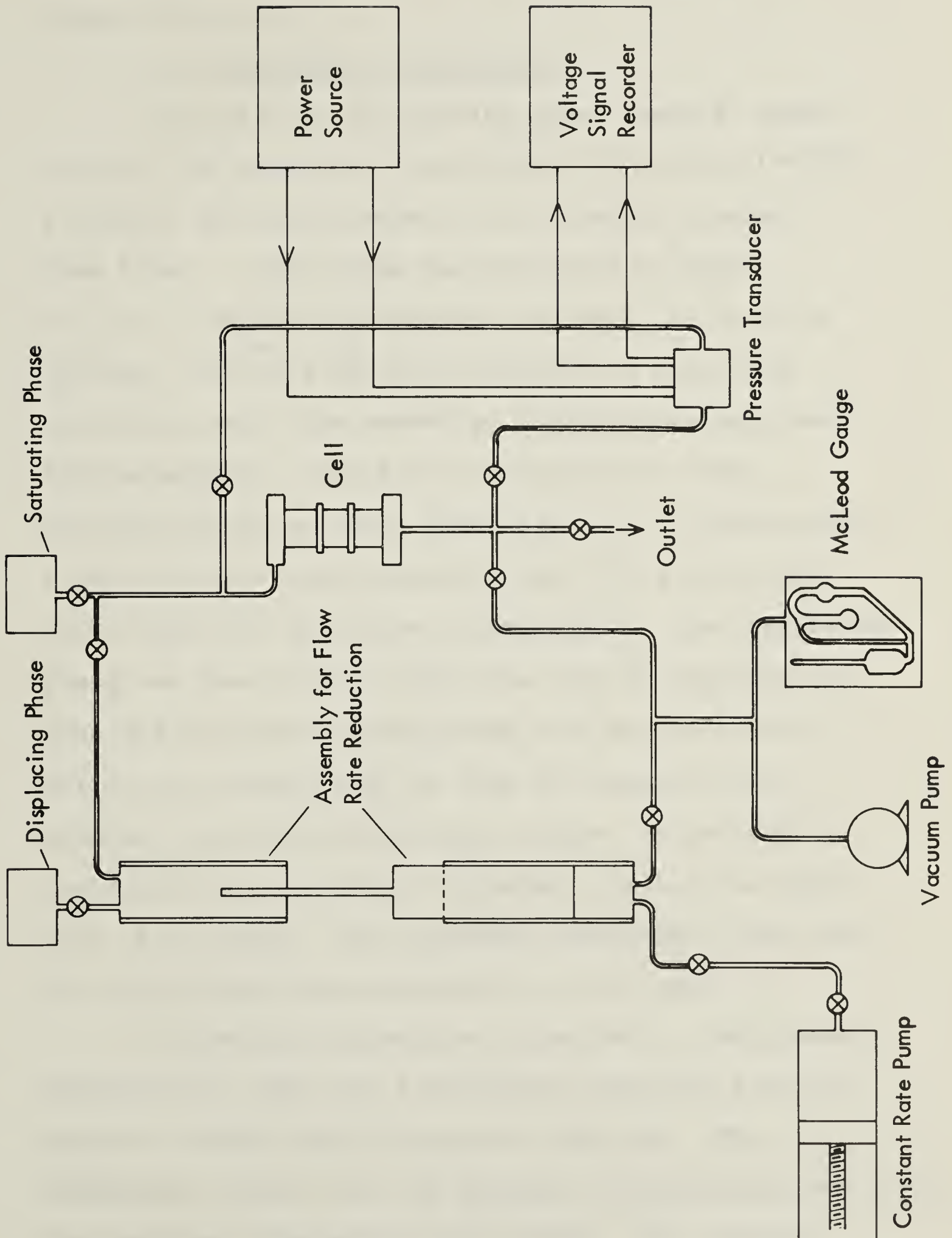


FIG. 3. FLOW DIAGRAM FOR CAPILLARY PRESSURE MEASUREMENT





was made of lucite and iso-octane was stored in a copper container.

### C) Experimental Procedure:

The cell was filled with glass beads to about 2/3rd of the height and was weighed accurately (within  $\pm 10$  mgm) and was attached to the freshly cleaned flow lines. The system was evacuated to about 0.2 to 0.3 mm [of Hg] absolute pressure for about 30 minutes, following which the saturating phase was allowed to enter the assembly, thereby attaining near 100% saturation. The fluid was allowed to flow through the system until about 150 c.c. of fluid (about 5 pore volumes) had passed the pack [This was a free flow, under the influence of gravity.]. The displacing phase was then injected into the cell by starting the pump and the pressure recording unit was switched on. During the earlier part of flow at constant rate, a constant pressure differential across the pack was recorded, until the fluid interface touched the upper part of the pack. This pressure differential was used for calculating the permeability of the pack.

A steplike increase was observed in the pressure differential, when the fluid-fluid interface tried to squeeze through the top layer of the pack. The difference between the two pressure differentials was taken as the capillary pressure of the system. The treated





beads had a tendency to float over brine solution, probably due to strongly adhering air films on their surfaces. A stainless steel wire mesh, together with a teflon ring-support and an additional supporting lucite tubular piece, were used to overcome this problem. The details are shown in Figure 4.

The cell was used with its longitudinal axis vertical. The iso-octane-brine interface, which was horizontal, gradually moved downwards, when the bead-pack saturated with brine, was displaced by iso-octane. In the reverse case, with the same set-up, the downward movement of iso-octane - brine interface was not possible due to density of brine being higher than that of iso-octane. This necessitated some alterations in set-up for the case of brine displacing iso-octane which was solved by holding the cell in an inverted position and modifying some of the flow lines.

In all tests, observations were taken with stainless steel mesh and all accessories in place.

The observations taken with each tests were, the weight of cell filled with beads, temperature, height of the bead-pack and pressure readings from voltage recorder chart. The procedures for calculating porosity ( $\Phi$ ), permeability (K), capillary Pressure, wettability number  $W'$  and apparent contact angle  $\theta'$  are presented in Appendix 3.



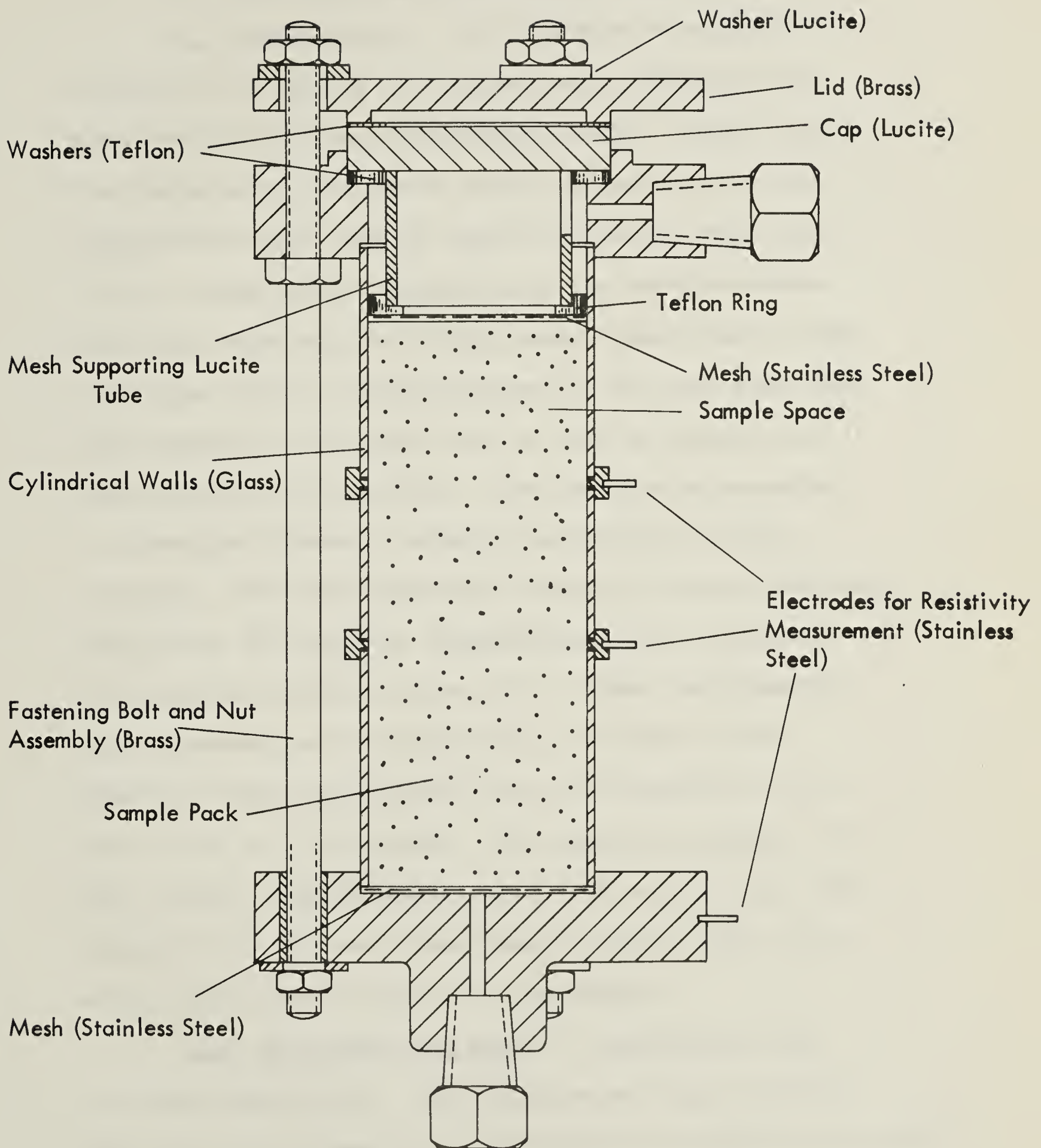


FIG. 4. CAPILLARY PRESSURE CELL





D) Description of Materials Used.

i) Glass Beads: - the beads were spheres or ellipsoids of nearly unit sphericity, provided by Microbeads Division, Catastrophe Corp., Toledo, Ohio. The beads were transparent under the microscope, but appeared whitish, due to their tiny size, when seen by the naked eye. According to the manufacturers, the beads were made of "high grade crown glass - soda lime type, with a silica content of no less than 68%". The composition of glass was of such a nature that it resisted wear or fracture. The beads were annealed in spherical shape in order to equalize internal stresses. The size range as stated by the manufacturer was 149 to 210 microns (manufacturer No. 710 and corresponding Ballotini No. 13). When the diameters were measured in the laboratory, of seven random spheres, they ranged from 120 to 240 microns with a mean value of 171 microns. The specific gravity of the freshly cleaned beads was 2.454 gms/cc which was reduced to 2.413 for glass beads treated with 4 gms of silicone per 500 gms of glass beads.

ii) Silicones and HMDS:- Dow-Corning 550 silicones were used. The fluids were clear, colourless with low viscosity, low volatility (Flash point 590°F) and were thermally stable up to 450°F. The Hexa-Methyl Disilazane was supplied by Applied Science





Laboratories Inc., P.O. Box 140, State College, Pa., and was also clear, colourless, with low viscosity, low volatility and toxicity and was thermally stable up to 400°F.

iii) Iso-Octane :- The iso-octane was Phillips 66, D-168 commercial Grade Iso-octanes. They had a boiling point of about 115 to 120°F., densities varying from 0.699 gms/cc at 68°F to 0.694 gms/cc at 80°F.; and the viscosities varying between 1.023 cp at 68°F to 0.964 cp at 80°F.

iv) Brine:- 7.5% brine was prepared by dissolving c.p. (chemically pure) sodium chloride (Fischer Scientific Co.) in distilled water. The brine showed a variation in viscosity from 1.082 cp at 70°F to 0.960 cp at 80°F. The density of the brine was 1.050 gms/cc at 75°F.



2.        TREATMENT OF GLASS BEADS TO ALTER THEIR  
          WETTABILITY.

A) Cleaning

The glass beads were cleaned before any fluid treatment. After rinsing the beads first with distilled water four to five times, and then with toluene for an equal number of times, the beads were immersed in a boiling chromic acid bath for two hours. They were then thoroughly washed with distilled water; oven dried at 250°F for three hours; cooled and stored in clean glass bottles.

B) Treatment with Silicone Fluids.

Glass beads weighing 500 gms were stored in a clean china dish. A watch glass, treated with sufficient silicone fluids was used to weigh controlled amounts of silicone 550 fluid in an electrical balance reading up to 0.1 mgm. In a glass pan (pre-treated with silicones), 250 cc's of iso-propanol (c.p.) was taken and the watch glass was immersed in the alcohol (iso-propanol) to transfer all silicones into solution. The fluids were stirred with a glass rod for four to five minutes. The glass beads were then slowly poured into the pan and the stirring was continued for the next thirty to forty minutes. The pan was placed in a fumes cupboard at 75°F and the iso-propanol was allowed to evaporate overnight. The pan was oven-dried at 250°F



for two hours following which, the glass beads were washed with petroleum ether for about 25 minutes and finally oven dried at 250°F for two hours. They were then stored in a clean, labelled glass bottle with wide mouth.

D \ Treatment with Hexamethyldisilazane (HMDS):-

This treatment was conducted along the lines suggested by Purnell (22). Glass beads weighing 200 gms were placed in a pyrex soxhlet extractor, supported from below by a stainless steel wire gauze. A reflux condenser was then fitted to the soxhlet extractor. 10 cc's of HMDS solution was dissolved in 150 cc's of petroleum ether in the heating flask and the extractor-condenser assembly was fitted to the flask. A 1/4" glass tubing, bent twice at 90° was used as a delivery tube for carrying any ammonia fumes evolved during HMDS-glass surface reaction. A 500 cc graduated cylinder carrying a solution of standardized sulphuric acid was used for determining the amount of ammonia evolved. The lower end of the delivery tube dipped into the  $\text{H}_2\text{SO}_4$  solution, and the upper end was fitted to the reflux condenser through a cork. Maximum heating rate (setting 100) provided by a 300 watt electrical hot plate and a fixed rate of water flow in the reflux condenser were used for all the treatments. Different amounts of treatments were obtained using different





periods of heating. At the end of the heating period, the heater was shut off and the delivery tube was disconnected from the condenser in order to avoid entry of acid into the flask due to suction caused during cooling, while the water was allowed to flow for some time longer. The assembly was then dismantled and any HMDS-petroleum ether solution in the glass beads was decanted back into the flask. The beads were removed and washed with petroleum ether and n-propanol. They were then oven dried for two hours at 250°F and stored. Since less than 10% of HMDS participates in the treatment, the same HMDS-petroleum ether solution was re-used with little addition of HMDS fluid. The amount of treatment was determined by titrating the sulphuric acid solution against NaOH using methyl orange as indicator. The sample calculations and results of all the treatments are presented in Appendix II.





### 3. MEASUREMENT OF OTHER PROPERTIES

The diameters of beads were measured using a travelling microscope, the height of bead pack for each test was determined using a Cathetometer. The densities of fluids and glass beads were determined using specific gravity bottles. The viscosities of fluids were measured using Ostwald's viscometers and constant temperature baths. The interfacial tensions for brine-iso-octane systems were determined using a Du Nouy Tensiometer and the corrections for bouyancy and ring size were made by the technique suggested by Zuidema and Waters (23). The transducer recorder calibration factors were tested using a mercury manometer and compressed air as a pressure source. The values of all relevant data, obtained as above, are presented in Appendix I.



## RESULTS

The observations made for the determination of apparent contact angles, for glass beads treated with silicone; for the cases of water (brine) displacing oil (iso-octane) and oil (iso-octane) displacing water (brine), are presented in Appendix 3, in Tables 1 and 2 respectively.

Similar data for glass beads treated with Hexamethyldisilazane (HMDS) are present in Tables 3 and 4 of the same appendix. These data were processed to obtain Wettability Numbers (W) and apparent contact angles  $\theta'$  as shown in Tables 5, 6, 7 and 8. The apparent contact angles thus calculated were plotted against appropriate values representing the extent to which the glass surfaces were treated with fluid. Figures 5 and 6 show such plots for the cases and silicone and HMDS treatment respectively.

The reproducibility of apparent contact angles in most cases was within  $5^\circ$ .

The final values of apparent contact angles  $\theta'$  and wettability Number W' as calculated in Tables 5, 6, 7 and 8 of Appendix 3 are summarised in Tables 1 and 2.

The specific surface area of the beads, as computed in appendix 1 is about 0.0143 square metres/gm of glass or 7.15 square meters/500 gms of glass. The



TABLE 1Effect of Silicone Treatment Upon Wetting Properties

		$\theta^*$ measured thro' oil phase		$\theta'$ measured thro' water phase		
Amount of Silicone Treatment	No. of Mono- layers	Oil Displacing Water		Water Displacing Oil		
gms/500 gms		W'	$\theta'$	W'	$\theta^*$	$\theta'$
Clean	- -	1	0°	0	90°	90°
		assume				
Clean	- -	0.925	22.3°	0.186	79.3	100.7°
0.025 gm	6	- - -		0.269	74.4°	105.6°
0.100 gm	24	0.812	35.7°	0.299	72.5°	107.5°
0.175 gm	42	0.483	61.1°	- - - - -		
0.264 gm	63	0.317	71.5°	- - - - -		
0.400 gm	96	- - -		0.403	66.2°	113.8°
0.500 gm	120	0.299	72.6°	6.376	67.9°	112.1°
0.500 gm	120	0.834	33.5°	- - - - -		
0.750 gm	180	0.236	76.4°	0.404	66.2°	113.8°
1.25 gm	300	0.143	81.8°	0.485	61.0°	119.0°
1.25 gm	300	- - -		0.513	59.2°	120.8°
1.50	360	0.232	76.6°	0.526	58.3°	121.7°
1.50	360	0.277	73.9°	- - - - -		
2.00	480	0.131	82.5°	0.525	58.4°	121.6°
3.00	720	- - -		0.471	61.9°	118.1°





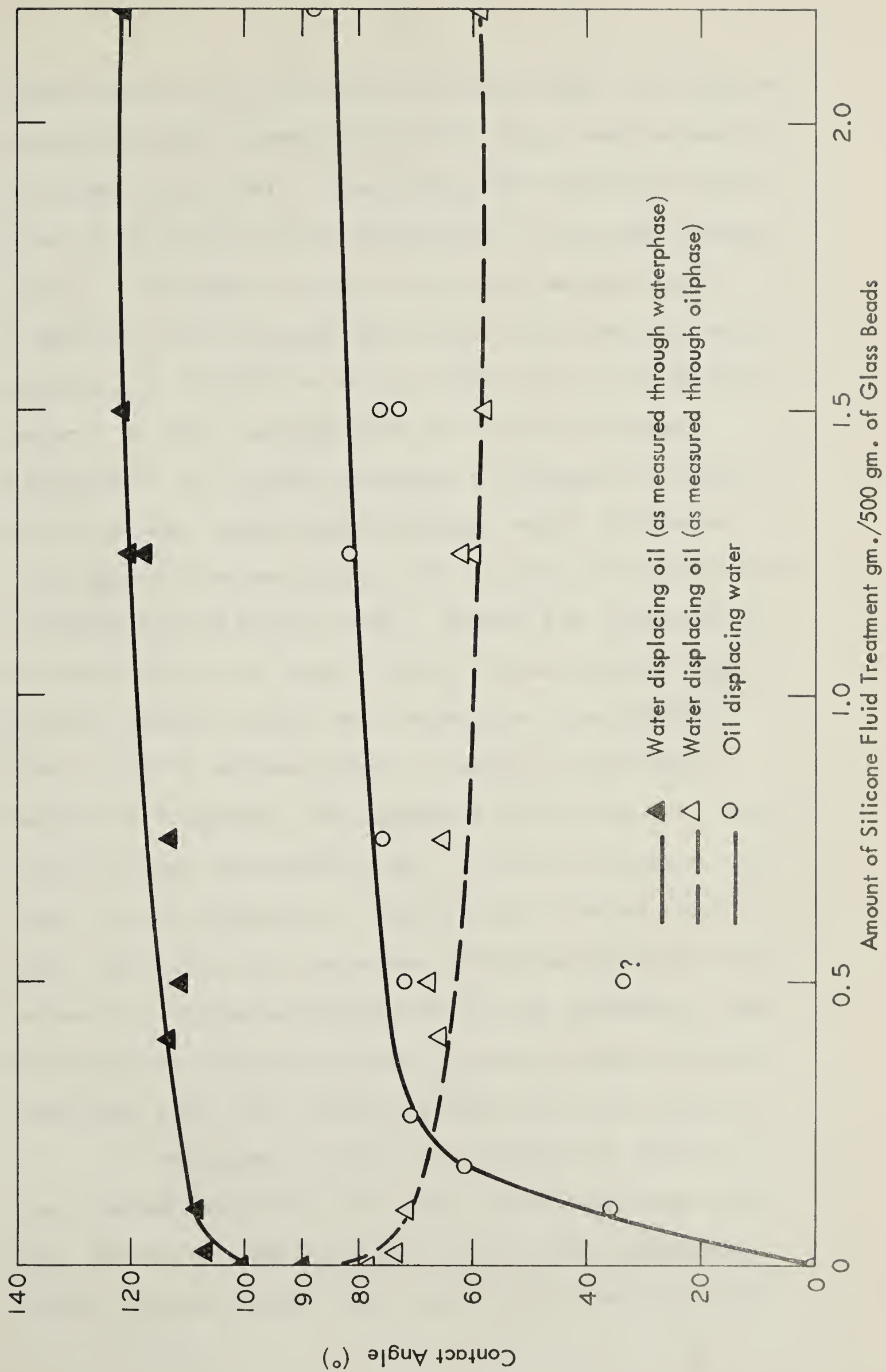


FIG. 5. EFFECT OF SILICONE TREATMENT ON CONTACT ANGLES



area occupied by a monolayer of silicones, as computed from force-area curves is about 1.7 sq. metres/mgm of silicone fluid (24). That meant that between 4 and 5 mgms of fluid should be sufficient to provide a monolayer. Treatments in excess of this amount (up to 3 gms/500 gms of glass) were tried but they failed to provide any imbibition of oil when the oil displaced water. It was observed that at higher silicone treatments, the beads indicated a tendency to cohere and form some random agglomerates, which indicated that quite an excess amount of silicone fluid remained sticking to the glass beads. Beyond the treatment of 0.5 gms/500 gms of glass (about 100 monolayers) the contact angles showed very anomolous behaviour in their contact angles, that is, after a particular amount of treatment, the excess fluids seemed to have little effect on wettability. It may be pointed out that the very purpose of washing the treated beads with n-propanol and petroleum ether was to remove any excessive, untreated fluid around the surfaces. The phenomenon of cohesion amongst treated beads probably indicates that this objective was not fully realised.

It was observed that the hysteresis shown by the treated beads was of a very large magnitude ( $20^{\circ}$  -  $40^{\circ}$ ) and at no time were the receding and advancing contact angles on the same side of  $90^{\circ}$  (neutral axis).



TABLE 2

EFFECT OF HMDS TREATMENT UPON WETTABILITY

Sample No.	Amount of HMDS treatment gms/500 gms	Hours of Treatment	Oil Displacing Water		Water Displacing Oil	
			W'	$\theta'$	W'	$\theta'$
#6	0.0417	1 1/2	.269	74.4°	.154	81.1°
#5	0.0820	2 1/4	.168	80.3°	.203	78.3°
#8	0.0835	2 1/2	.155	81.8°	.252	75.4°
#3	0.194	3 1/2	.272	74.5°	.238	76.2°
#4	0.194	3 1/2	.149	81.4°	.317	71.5°
			.254	75.5°		108.5°
#7	0.2045	3 3/4	0.380	67.7°	0.245	75.8°
#2	0.288	7	.150	81.4°	0.279	73.8°
			.254	75.6°		106.2°
#1	0.312	12	.1081	83.8°	0.336	70.4°
						109.6°

 $\theta^*$  Measured thro' oil phase $\theta'$  Measured thro' water phase





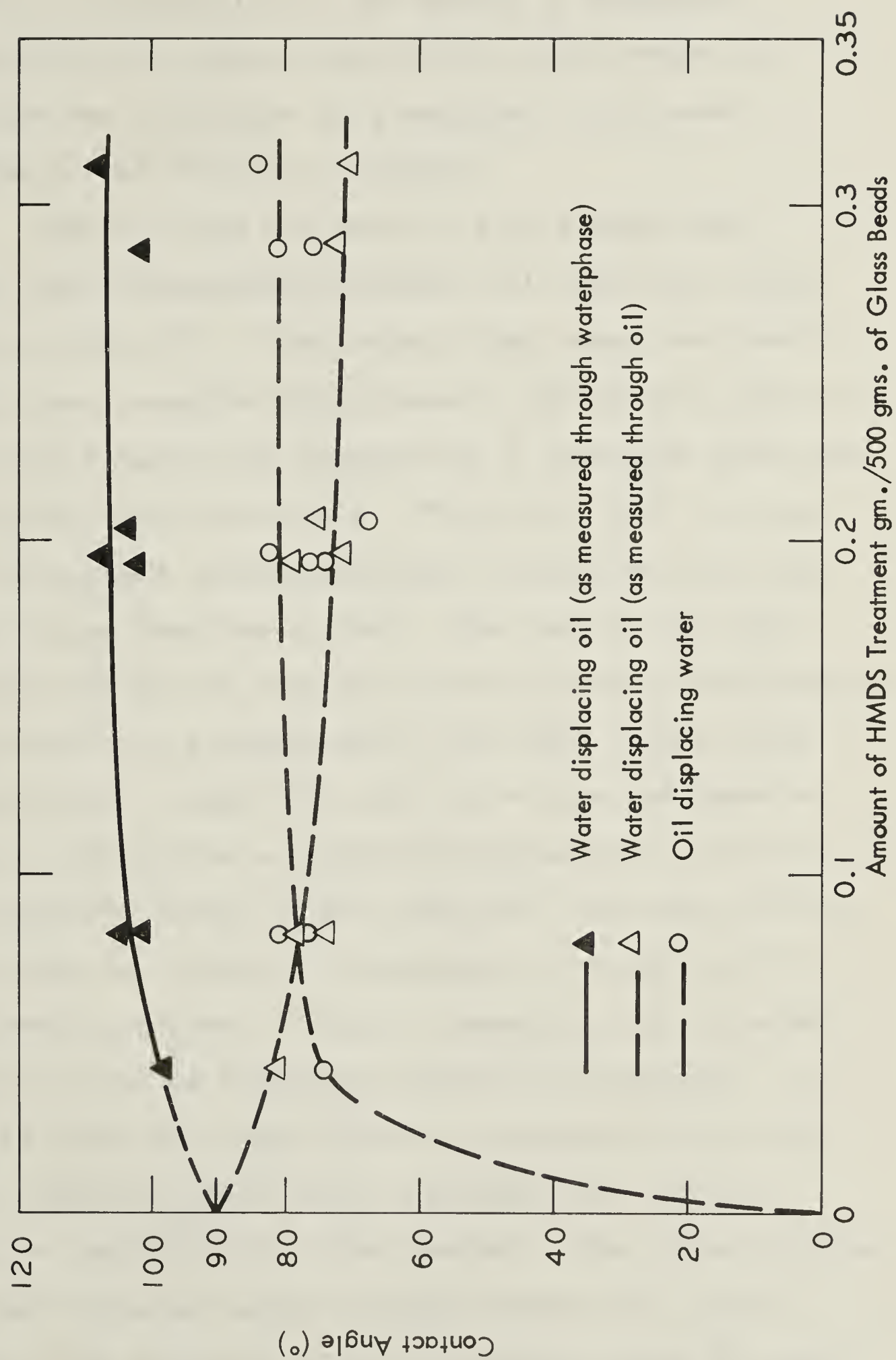


FIG. 6. EFFECT OF HMDS TREATMENT ON CONTACT ANGLES



That is, irrespective of the amount of treatment imparted or the cleanliness of the fresh beads, at no time was imbibition or a negative displacement pressure (differential) recorded.

Benner, Dodd and Bartell (25) suggest that water may spontaneously displace oil when both angles are less than  $90^\circ$ . They report that under near-static conditions, negative displacement (imbibition) pressures for porous media were measured by a technique described by Bartell and Benner (26). They state that "In none of the systems investigated did oil spontaneously displace water from the silica". The lack of any spontaneous imbibition observed in the present investigations may be partially explained in the light of the above observations. Apart from the above reported measurement of imbibition or negative displacement pressures, an extensive survey of the available literature failed to reveal any report of measurement of negative displacement pressures. Table 3 summarises the reported results of fluid treatment wettability behaviour. It may be noted that the method of determination of contact angles in these cases was either the Sissle drop or the Capillary "rise" method. The contact angles of the untreated samples ranged between  $45^\circ$  and  $90^\circ$ . None of the reported values of contact angles on glass exceeds  $125^\circ$  except the ones reported by Newcombe et al (27)



TABLE 3

Effect of Silicone		Treatment on Contact Angles on Glass Surfaces (as reported in literature)				
Source	Budhiraja (28)	Newcombe et al (29)	Coley et al (30)	Spitze et al (23)		
Fluid	Dri-Film SC-87	DC - 1107	GE No 99	Organo siloxanes at 200°F		
	Vol. Conc. in C <sub>6</sub> H <sub>6</sub> %	Mgm/gm	No of layers	θ	Wt%	
	θ				θ	
	0	0	0	45°+15	0	
	.00125	.0125	.47	62 +10	.002	
	.00250	0.025	0.94	85 +10	.02	
	.0525	0.05	1.88	108 +10	.2	
	1.0525	0.10	3.76	140 +10	2	
		1.0	37.6	157 +5		
Method	Capillary tube	Sissle drop	Capillary	Sissile drop		
Other Phase	Air	Soltrol	Air	Air		

All values of θ are those measured through water phase.





who used the Sissile drop method on a water-soltrol system. This indicates a relatively weak adhesion tension between the treated surface and the oil phase.

In the present investigations, the largest contact angles obtained were slightly lower than  $122^\circ$ . Due to the low values of adhesion tension and the complications of geometry it appears that in the near neutral wettability conditions, the method is not very sensitive.

Since no receding angle greater than  $90^\circ$  and no advancing angle less than  $90^\circ$  could be observed, it appears that for the cases of near-neutral wettability, showing great hysteresis effect, the purpose served by the method is nothing more than a qualitative indication of preferential wettability.

In the near-neutral wettability cases the preferential wettability may possibly be indicated in the following way. If the contact angle for the case of oil displacing water as measured through the water phase is less than the contact angle measured through the oil phase in case of water displacing oil; the surface is preferentially oil wet.

The behaviour of all the systems reported above, as well as the results of the present investigations of wettability indicate that the glass surface wett-



ability can be changed by applying different amounts of silicone fluid. As indicated by the present studies further increases in the preferential wettability through the oil phase are not likely to be produced by applying treatments in excess of about 60 equivalent monolayers. Even this figure appears to be too high. Newcombe et al (23) report that upon increasing the treatment with silicone, in terms of equivalent monolayers, from 2.76 to 37.6 the contact angles changed from  $140^{\circ} \pm 10^{\circ}$  to  $157^{\circ} \pm 5^{\circ}$ . In the light of their findings, the optimum value of treatment of 60 equivalent monolayers may not be too unreasonable.

The HMDS treatment showed a maximum contact angle of  $110^{\circ}$  with all the values lying within a narrow region. This indicated that HMDS treatments in excess of 0.1 gms/500 gms of glass beads had very little effect upon contact angles. In this investigation the application of treatment was dependent upon a reaction which occurred at elevated temperatures (the boiling point of ether is  $90^{\circ}\text{C}$ ). Consequently the only way in which the amount of treatment could be altered was by varying the length of time, the system remained at the elevated temperature. Because of the procedure used, it was not possible to precisely control the amount of treatment.

The plot of duration of reaction vs amount of



treatment is presented in appendix 2. This plot is not discussed here, since no values of apparent contact angles in the water wet range could be observed and the procedure provides a rather poor control over the amount of fluid treatment in the lower range.





### RECOMMENDATIONS

A method of dynamic imbibition test, coupled with the concepts of displacement (capillary) pressure should be able to remove the draw backs encountered with the current experimental technique of the displacement test. The dynamic imbibition test may be standardized in such a way that the pressures required for displacement of the first drop of fluid from the core be determined. Such a method would exhibit a flow behaviour, which would be closer to the actual displacement phenomenon.

Different solvents to completely wash away any amount of un-adsorbed HMDS and silicones on the glass surfaces should be studied and perfected.

The reaction of HMDS with glass surfaces should be further investigated and the feasibility of controlling the amount of HMDS treatment, so as to obtain contact angles in water-wet range, needs further study.



### CONCLUSIONS

1. The technique used for application of silicone fluids to glass surfaces seems quite effective for the alteration of wettability to a desired degree.
2. Controlled and small amounts of silicone fluids can be used to obtain values of apparent contact angles up to  $122^\circ$  with the brine - iso-octane - glass system.
3. Treatment of glass surfaces with amounts of silicone fluid in excess of 60 equivalent monolayers fails to produce appreciable changes in the values of contact angles. Such extensive treatment should be avoided if the glass beads so treated are to be used in flow tests; since it merely causes agglomeration.
4. The displacement pressure technique has been modified so as to permit the measurement of capillary pressures at different conditions of temperatures and pressures. However, more modifications seem necessary for the technique to detect and record imbibition phenomena.
5. Since advancing angles less than  $90^\circ$  and receding angles more than  $90^\circ$  could not be observed with the capillary pressure technique, the technique appears to be unsuitable for near neutral wett-



ability ranges. A combination of the imbibition test and the capillary pressure technique is recommended. This would combine the advantages of both systems.

6. Apparent contact angles in the water-wet range could not be obtained with hexamethyl-disilizane, however, for the surfaces treated, the maximum advancing angles through water was  $110^{\circ}$ . Increase in amount of treatment above 0.1 gms/500 gms seemed to have little effect. In view of this, the possibility of improvement in the technique should be investigated. Attempts should be made to control the amount of treatment more precisely so as to obtain apparent contact angles in the water-wet range.





NOMENCLATURE

A,B	Fluid phases
A <sub>T</sub>	Adhesion Tension (dynes/cm)
d	Diameter of particles (cm)
g	Acceleration due to gravity (cm/sec <sup>2</sup> )
h	Height of liquid rise in capillaries (cm)
K	Permeability (darcies or cm <sup>2</sup> )
o	Subscript for observed
P <sub>c</sub>	Capillary pressure (gm/cm <sup>2</sup> )
P <sub>l</sub>	Pressure differential across the core gm/cm <sup>2</sup>
r	Radius of capillary tube (cm) or subscript for reference condition.
S	Solid phase
W	Wettability number or index
W'	Modified wettability index
x	Ratio of actual surface area of a rough plane to its apparent plane area.
Δρ	Difference in densities (gms/cm <sup>3</sup> )
θ	Contact angle (°)
θ'	Apparent contact angle (°)
θ̄	Measured contact angle (°)
σ	Interfacial tension dynes/cm
Φ	Porosity (% or fraction)



## BIBLIOGRAPHY

1. Wenzel, R.N.  
Resistance of Solid Surfaces to Wetting by Water.  
Ind. & Engg. Chem. Vol. 28 (8) pp 988-994  
(1935)
2. Cassie and Baxter  
Trans. Faraday Soc. (1944) 40, p 546
3. Adam, N.K.  
"Principles of Penetration of Liquids into  
Solids"  
Disc. Faraday Soc. No. 3 (1948) pp 5-11
4. Holland, L.  
"Properties of Glass Surfaces",  
John Wiley & Sons, New York (1964)
5. Pohlack, H. and Wendler, S.  
Jenaer Jahrbuch, p. 41, VEB Carlzeiss Jena (1958)
6. Holland, L. - op cit
7. Purnell, H.  
"Gas Chromatography"  
Wiley - (New York) 1962 pp 235-237
8. Spitze, L.A. and Richards, D.O.  
"Surface Studies of Glass; Part I Contact Angles"  
J. App. Physics 18 (1947) pp 904-911
9. Holbrook, O.C. and Bernard, G.G.  
"Determination of Fractional Wettability in Oil  
Field Cores by Dye Adsorption"  
Trans. AIME 213 pp 261-266 (1958)
10. Brown, R.J.S. and Fatt, I.  
"Measurement of Fractional Wettability of Oil  
Field Rocks by Nuclear Magnetic Relaxation  
Method"  
Trans. AIME 207 (1956) pp 262-268
11. Bobek, J.E.; Mattax, C.C. and Denkas, M.O.  
"Reservoir Rock Wettability - Its Significance  
and Evaluation".  
Trans. AIME 213 (1958) pp 155



## BIBLIOGRAPHY

12. Leverett, M.C.  
     "Capillary Behaviour in Porous Solids"  
     Trans. AIME 142 (1941) pp 152-169
13. Plateau, J.A.F.  
     "Capillary Pressure in Packing of Uniform Spheres"  
     Smith Instt. Ann. Reports 1863-1866 as  
     quoted by Champion and Dary "Properties of  
     Matter" New York, 1937, Prentice Hall,  
     pp 99 - 101.
14. Carman, P.C.  
     Soil Sci. 52 (1941) pp 1-6
15. Leverett, M.C.  
     "Flow of Oil-Water Mixtures Through Un-  
     Consolidated Sands"  
     Trans. AIME 132 (1939) pp 149-171
16. Bartell, F.E. and Osterhof, H.J.  
     "Determination of the Wettability of a Solid  
     by a Liquid"  
     Ind. and Engg. Chem. 19 (1927) pp 1277-83
17. Slobod, R.L. and Blum, H.A.  
     "Method for Determining Wettability of  
     Reservoir Rocks"  
     Trans. AIME 195 (1952) pp 1-4.
18. Faris, SR and Whalen, J.W.  
     Discussion of Paper by Slobod and Blum  
     (16 above) ibid page 4.
19. Adam, N.K. - op cit.
20. Calhoun, J.C. (Jr.)  
     "Criteria for Determining Rock Wettability"  
     Oil Week, May 10, 1951, pp 151-154
21. Pohak and Wendler - op cit





## BIBLIOGRAPHY

22. Zuidema, H.H. and Waters, G.W.  
"Ring Method for Determination of Interfacial  
Tension"  
Ind. & Engg. Chem. Anal. 13 (1941) pp 312-313
24. Fox, H.W.; Taylor, P.W. and Zisman, W.A.  
"Polyorganosilanes - surface active Properties"
25. Benner, F.C.; Dodd, C.G. and Bartell, F.E.  
"Evaluation of Effective Displacement Pressures"  
API - Drilling and Production Practice (1942)  
pp 169 - 177
26. Bartell, F.E. and Benner, F.C.  
"Adsorption at Solid-Liquid Interfaces"  
J. Phys. Chem. 46 (1942).
27. Newcombe, J.; McGhee, J. and Rzasa, M.J.  
"Wettability Versus Displacement in Water  
Flooding in Unconsolidated Sand Columns",  
Trans. AIME Vol. 204 (1955) pp 227 - 232
28. Budhiraja, J.L.  
"Effect of Wettability on Oil Recovery"  
M.S. Thesis, University of Alberta, 1963.
29. Newcombe, et al - op cit
30. Coley, F.H.; Marsden, S.S. and Calhoun, J.C. (Jr.)  
"A Study of Effect of Wettability on the  
Behaviour of Fluids in Synthetic Porous Media"  
Prod. Mo. June 1956, pp 29 - 45.
31. Spitze et al - op cit



## APPENDICES



## APPENDIX I

### DETERMINATION OF MISCELLANEOUS PROPERTIES

#### 1. DESCRIPTION OF BEADS:

Diameters of different samples of clean untreated beads were measured and a mean value of 0.0171 centimeter was obtained. Values of individual measurements are shown under the column Small beads in Table I, Appendix I of Part 1 in this thesis.

From the mean diameter of 0.0171 cm, the specific surface was calculated as follows. Since all particles are spherical, the specific surface per unit volume of glass is

$$\frac{n(\pi d^2)}{n(\frac{1}{6}\pi d^3)} = \frac{6}{d}$$

or approximately  $\frac{6}{.0171}$  i.e. 350 sq cm per c.c. The specific gravity of clean beads is 2.442 and hence the specific surface area in terms of square metres per gm of glass beads is .0143 sq m/gm. This is equivalent to 7.15 sq m/500 gms of glass beads.

The density of the HMDS treated beads was almost the same as that of untreated clean beads but in case of silicone treated beads, a sample treated with 4 gms of silicone/500 gms of glass beads showed a density of 2.413 gms/c.c.

#### 2. PROPERTIES OF FLUIDS:

a) Iso-octane: The density of iso-octane was found





to be 0.6992 gms/c.c. at 68° F and 0.6942 gms/c.c. at 80°F. The viscosity was 1.023 centipoise at 68°F and 0.964 centipoise at 80°F.

b) Brine: The density of brine at 68°F was 1.0499 gms/c.c. and reduced to 1.0480 gms/c.c. at 80°F. The viscosity values at 68°F and 80°F were 1.083 cp. and 0.980 c.p. respectively.

c) Interfacial Tension: The values of interfacial tension between Brine and Iso-octane after corrections for ring size and buoyancy effect were 45.86 dynes/cm at 71°F. and 41.60 dynes/cm at 79.5°F.

The appropriate values of these properties at different temperatures were interpolated from the data described above.

### 3. CALIBRATION OF PRESSURE TRANSDUCER AND RECORDING DEVICE

Using air as the pressure source and a mercury manometer as the pressure measuring device the signals of pressure transducers, as recorded by the Visicorder and Dynograph were calibrated. For input voltage value of 15 volts, the observed calibration was 1.3095 cm of deflection per psi. Corresponding figures from those reported for the transducer and viscorder in manufacturer's literature were 1.252 which agreed within 4%. Since the manometer was not very sensitive, the calibration factors provided by the manufacturers were used.



APPENDIX IIDETERMINATION OF AMOUNT OF HMDS TREATMENT

On reaction with glass surface, one molecule of HMDS  $\left( (\text{CH}_3)_3\text{Si} - \text{NH} - \text{Si} (\text{CH}_3)_3 \right)$  liberates one molecule of ammonia ( $\text{NH}_3$ ). The molecular weight of HMDS is 161 and that of ammonia is 17.

The ammonia dissolves in  $\text{H}_2\text{SO}_4$  to form  $(\text{NH}_4)_2\text{SO}_4$ . Therefore, 1 litre of normal solution of  $\text{H}_2\text{SO}_4$  will be consumed by 17 gms of  $\text{NH}_3$  liberated from 161 gms of HMDS; or 1 cc of N -  $\text{H}_2\text{SO}_4$  will be consumed by ammonia liberated from 0.161 gms of HMDS.

In the titration data, as presented in Table 1, the  $\text{H}_2\text{SO}_4$  unreacted was titrated by NaOH solution, using methyl-orange as the indicator. The normality of NaOH was N/10.15 while that of  $\text{H}_2\text{SO}_4$  was N/10.56.



TABLE I

DETERMINATION OF AMOUNT OF HMDS TREATMENT

Sample No.	Hours of Heating	Wt. of glass beads. (gm)	Vol of $H_2SO_4$ added(c.c.)	Amount of NaOH for back titration(c.c.)	Equivalent N - $H_2SO_4$ consumed (c.c.)	Treatment (gms/500 gms of beads)
1	12	500	75.0	52.3	1.951	0.312
2	7	500	75.0	54.0	1.801	0.288
3	3 1/2	250	1000	90.0	1.212	0.194
4	3 1/2	250	100.0	90.0	1.212	0.194
5	2 1/4	250	100	93.5	0.512	0.082
6	1 1/2	200	100	95.0	0.260	0.0417
7	3 3/4	200	100	91.0	1.280	0.2045
8	2 1/2	200	100	94.0	0.521	0.0835





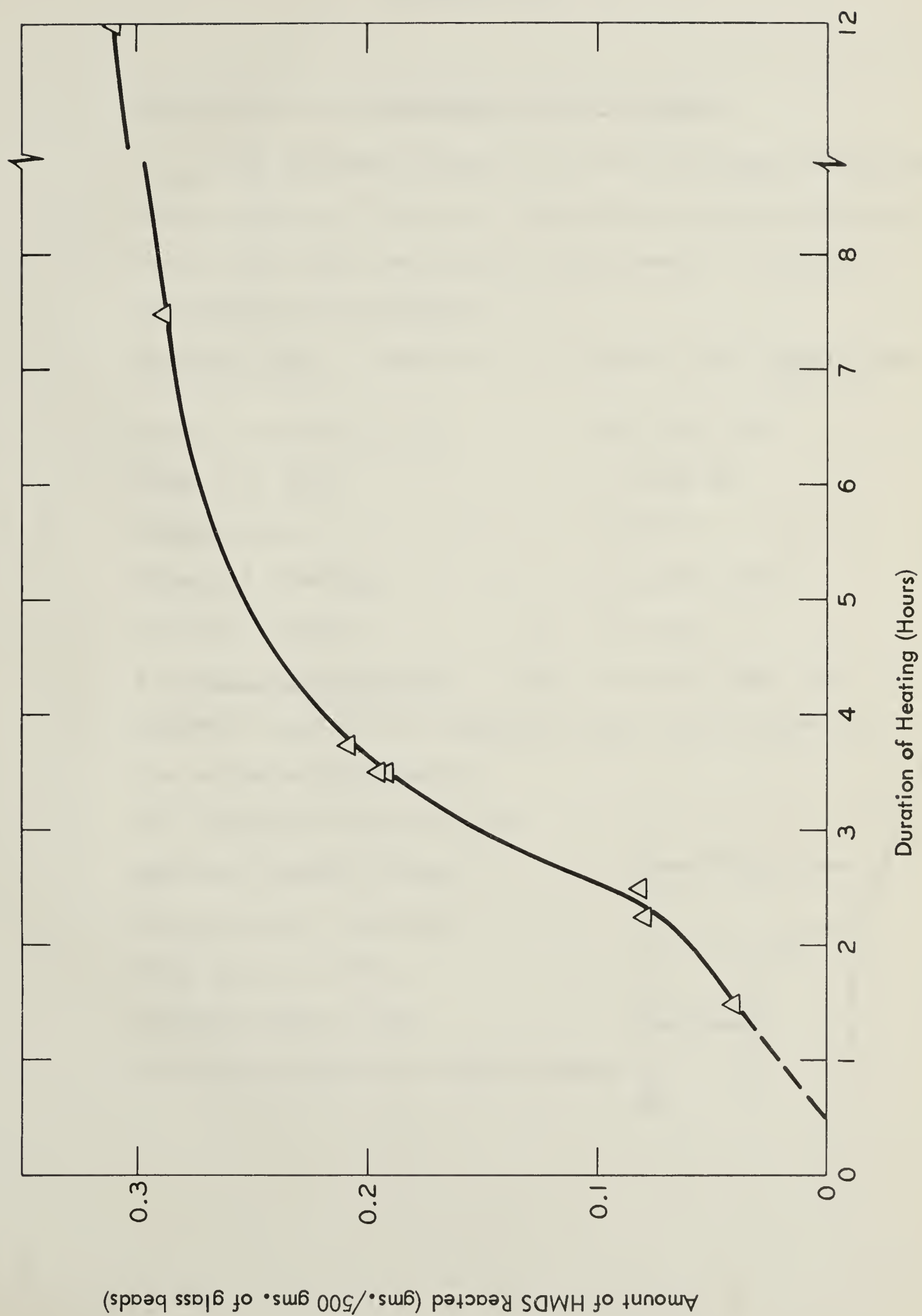


FIG. 7. EFFECT OF DURATION OF HEATING ON THE REACTION OF HMDS WITH GLASS SURFACE



APPENDIX IIIDetermination of Apparant Contact Angles

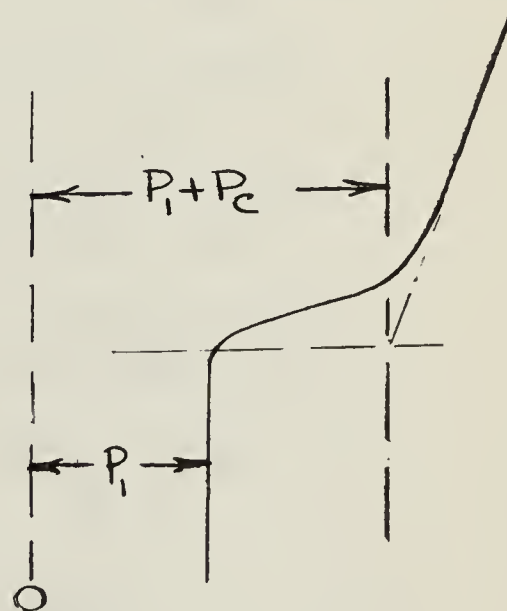
The measured properties were the weight of pack and cell, height of pack, the temperature and the pressures before and after capillary displacement. A sample calculation is presents.

Observed Data (Sample No. 1, Table 4, Oil displacing Water)

Weight of packed cell	1483.505 gms
height of pack	- 3.490 cm
Temperature	75.2°F
Pressure Readings	3.83 and 3.98
Voltage Applied	= 10 volts

a) Capillary pressure - It may be noted that the general shape of the pressure chart is as shown in the accompanying sketch.

The pressure traces show a gradual increase after displacement and hence they must be extra-polated back to the starting position of displacement.





For the above data (for 10 volts), the deflection can be computed as follows:

The calibration factor of Transducer = 136.3 Microvolts/volt/Psi

The calibration factor of Galvanometer = 2.41 Millivolts/inch

The calibration factor for the recorder at 10 volts input voltage

$$= 10 \times 136.3 \times 2.41 \times 2.54 \times 10^{-4}$$

$$= 0.835 \text{ cm/psi}$$

The capillary pressure = 0.15 cm  
= .0764 psi

b) Interfacial Tension:- From the values of interfacial tension given in appendix 1, at 75.2°F,  
=44.80 dynes/cm.

c) Porosity:-

Weight of pack = 1483.505 - 1349.525 gms  
= 133.980 gms

Height of pack = 12.21 - 3.49  
= 8.72 cm

Volume of pack = 10.463 x 8.72  
= 91.237 c.c.

Apparant Density = 133.980/91.237  
=1.468 gms/c.c.

Porosity =  $\frac{Q_g - Q_a}{Q_g}$   
= 39.84%





d) Permeability:- Incorporating pump rate of 300 c.c. per hour and other details, the relationship is

$$K = \frac{.5378 \mu L_{(cp)} (cm)}{\Delta P_{atm}} \text{ millidarcies}$$

Viscosity of brine at 75.2°F = 1.019 cp

Pressure Differential = .1329 atm

Height of pack = 8.72 cm

Permeability = 36.0 md

e) Apparant Contact Angle:- The product

$$\frac{\Delta P}{6_{IT}} \sqrt{K/\phi} \text{ from the above is } 1.662 \text{ where as that}$$

for the cleanest possible beads (assumed contact angle = 0°) is 15.311. From these, the wettability index

$$\cos \theta = 1.662/15.311 = 0.1081$$

$$\text{Apparant Contact Angle} = \cos^{-1} 0.1081 = \underline{83.8^\circ}$$

The observed data for the 4 cases studied are presented in Tables 1 to 4 and the calculation of contact angles are shown in tables 5 to 8. These data are summarized in Tables 1 and 2 of the main text.



TABLE 1Observations Sheet

for Determining Wettability in the case of  
Oil Displacing Water on Silicone Treated Beads

Amount of Silicone on beads gms/500gms	Pressures* $P_l$ (cm)	$P_l + P_c$	Wt. gms.	ht. cm.	T °F
Freshly cleaned	1.68	2.30	1552.67 +	1.640	73.5°
	1.82	2.43	1539.09	0.835	74.7°
0.175g	2.96	3.39	1516.57 -	2.92	72.1°
0.1g	2.90	3.60	1519.47 -	2.92	73°
0.5g	2.84	3.56	1515.03 -	3.1	73.5°
0.75g	2.82	3.02	1515.10 -	3.15	75.5°
1.25g	2.89	3.01	1513.22 -	3.20	77°
2g	2.22	2.23	1512.91	3.15	75°
1.5g	2.16	2.20	1505.78 -	3.20	79.5°
4.0g	3.06	3.06	1511.35 +	1.30	80°
.264g	3.80	4.23	1486.105 -	3.265	77°
	(MV)				
3g	4.19	4.225	1463.1 -	4.715	76°
0.5g	3.63	4.180	1425.8 -	7.115	77°

\* The last three are readings in MV from Dynograph.

\*\* negative sign indicates the difference between top of  
cell and the top of pack in other cases height of  
extension piece above top is noted.



TABLE 2Observations Sheet

for Determining Wettability in the Case of  
Water Displacing Oil on Silicone Treated Beads

Amount of Silicone Treatment gms/500gms	Pressure Readings		wt. (gm)	ht. (cm)	T (°F)
	(cm)	(cm)			
Fresh	3.19	3.39	1519.300	-3.90	77°F
1	4.13	4.81	1495.330	+0.91 cm	71°F
4	4.60	4.30	1494.400	+0.725 cm	74.3°F
3	4.18	4.90	120.86*	+0.495 cm	72°F
2	4.16	4.89	1496.450	-3.195 cm	73.2°F
1.5g	4.43	5.03	1486.120	-3.755	74.5°F
1.25	4.03	4.79	139.885*	-3.315	75°F
0.75	4.06	4.80	1490.370	-3.440	74°F
0.50	4.09	?4.53 ?4.61	;495.610	-3.295	73.8°F
0.10	4.14	4.56	1493.100	-3.430	71.5°F
0.02	4.03	4.41	1485.500	-3.340	72.2°F
Fresh	4.04	4.04	1481.125g	-3.810	75°F
0.4	4.01	4.58	1479.275	-3.615	74°F

\* weight of the pack.





TABLE 3

Observations Sheet  
for Determining Wettability  
in the case of Water Displacing Oil on  
HMDS Treated Glass Beads

Sample No.	Pressure (MV)		Wt gms.	ht cm.	T
1	4.21	4.71	1486.03	3.38	74°F
2	3.91	4.31	1488.51	4.56	73°F
3	3.93	4.39	1487.53	3.38	73°F
4	3.62	3.98	1413.45	7.985	70.8°F
5	3.84	4.37	1411.95	8.065	76°F
6	3.66	3.95	1428.04	6.97	76°F
7	3.91	4.26	1398.92	8.915	76°F
8	3.82	3.92	1459.8	5.150	76°F



TABLE 4Observation Sheet

for Determination of Wettability in the Case of

Oil Displacing Water

on HMDS Treated Beads

Sample No.	Pressure (cm)		wt. gms.	ht. cm.	T
1	3.83	3.98	1483.505	-3.490	75.2°F
7	3.78	4.30	1484.520	-3.305	76°F
6	3.80	4.17	1483.55	-3.55	74.8°F
5	3.77	4.00	1484.528	-3.40	75°F
4	3.78	3.97	1484.61	-3.54	75°F
2	3.81	4.00	1483.795	-3.600	74.8°F
4	4.10	5.07	1470.02	-4.58	73°F
3	5MV	5.8MV	1463.0	-4.73	74°F
8	4.55MV	4.80MV	1425.5	-7.085	68.5°F
2	4.20MV	4.60MV	1477.22	-3.67	69.0°F



TABLE 5

Determination of  
Apparent Contact Angles  
 in the Case of Water Displacing Oil on  
 Silicone Treated Beads

Amount of Silicone Treatment gms/500 gms	$\Delta P$ Psi	$\gamma_{IT}$ dynes/cm <sub>1</sub>	$\phi$	k md	$\cos \theta$	$\theta$ (°)
Fresh	.102	42.90	32.15	46.15	.186	79.3
1.250	0.35	45.78	36.92	34.89	.485	61°
3g	0.3665	45.29	42.53	33.85	.471	61.9°
2g	0.3716	44.70	38.25	35.73	.525	58.4°
1.5g	.3767	44.31	39.15	31.15	.526	58.3°
1.25g	.3869	43.85	38.43	35.95	.513	59.2°
.75g	.3055	44.09	39.63	35.54	.404	66.2°
.5g	.2647	44.41	38.38	35.88	.376	67.9°
.1g	.2138	45.48	38.66	36.90	.2999	72.55°
.025g	.1935	45.19	40.30	37.31	.269	74.4°
Fresh	-	43.85	38.99	34.05	-	90°
0.4g	.2953	44.31	41.12	35.29	.403	66.2°





TABLE 6

Determination of Apparant Contact Angles  
for Silicone Treated Beads in the Case of  
Oil Displacing Water

	$\Delta P_c$ Psi	$\sigma_{IT}$ dynes/cm	$\Phi$ $q_0$	k md	$\cos \theta$	$\theta$ (°)
Freshly cleaned	0.474	44.55	36.37	75.12	1 assume	0°
" "	0.470	44.00	36.42	63.66	0.925	22.3°
0.175g	0.328	45.25	34.61	35.98	0.483	61.1°
0.1g	0.535	44.80	33.58	36.37	0.812	35.7°
0.5g	0.550	44.55	33.86	36.16	0.834	33.5°
0.75g	0.153	43.62	33.42	35.38	0.236	76.4°
1.25g	0.092	42.90	32.54	33.65	0.143	81.8°
2g	0.0076	43.85	34.02	45.81	0.131	82.5°
1.5g	0.137	41.69	36.90	43.10	0.232	76.6°
0.264g	0.2185	42.90	40.44	36.40	.317	71.5°
3g	0.017	43.39	40.24	29.04	.0219	88.75
4g	0.022	42.42	38.87	23.40	.0268	88.45
0.5g	0.268	42.90	42.34	22.60	.2986	72.6°
1.5g	0.1956	42.65	40.07	34.42	.277	73.9



TABLE 7

Determination of  
Apparant Contact Angles  
 for HMDS Treated Beads  
 in the Case of Water Displacing Oil.

Sample No.	$\Delta P$ Psi	$\sigma^T$ dynes/cm	$\phi$	$k_{md}$	$\cos \theta$	$\theta'$ (°)
1	.2446	44.31	38.96	33.75	.3360	70.4°
2	.1956	44.80	37.79	36.10	.2789	73.8°
4	.2250	44.80	38.77	36.30	.3172	71.5°
3	.1761	45.85	40.74	39.00	.2383	76.2°
6	.1076	43.39	41.02	37.25	.1539	81.1°
5	.1418	43.39	41.31	42.78	.2028	78.3°
7	.1712	43.39	41.19	33.35	.2448	75.8
8	.1956	43.39	38.81	29.36	.2527	75.4°



TABLE 8

Determination of  
Apparant Contact Angles  
 for HMDS Treated Beads in the  
 Case of Oil Displacing Water

Sample No.	$\Delta P$ Psi	<del>600</del> dynes./cm	$\phi$	k md	$\cos \theta$	$\theta$ (o)
1	.0764	43.80	39.84	36.0	.1081	83.8°
7	.2644	43.40	40.61	36.85	.3796	67.7°
6	.1881	43.95	39.38	36.30	.269	74.4°
5	.1170	43.86	39.96	37.10	.168	80.3°
4	.0966	43.86	38.97	36.40	.149	81.4°+
2	.0966	43.95	38.93	35.95	.1497	81.4°-
4	.1932	44.80	38.35	30.20	.2504	75.5°
3	.195	44.30	40.53	35.05	.272	74.5°
8	.122	46.95	42.00	35.0	.155	81.1°
2	.195	46.70	41.51	36.26	.254	75.6°







B29839